Inhibition of Dynamin Mediated Endocytosis by the *Dynoles*—Synthesis and Functional Activity of a Family of Indoles

Timothy A. Hill,[†] Christopher P. Gordon,[†] Andrew B. McGeachie,[‡] Barbara Venn-Brown,[†] Luke R. Odell,[†] Ngoc Chau,[‡] Annie Quan,[‡] Anna Mariana,[‡] Jennette A. Sakoff,[§] Megan Chircop (nee Fabbro),[‡] Phillip J. Robinson,[‡] and Adam McCluskey*,[†]

Chemistry, School of Environmental and Life Sciences, The University of Newcastle, University Drive, Callaghan NSW 2308, Australia, Cell Signaling Unit, Children's Medical Research Institute, The University of Sydney, 214 Hawkesbury Road, Westmead NSW 2145, Australia, Department of Medical Oncology, Calvary Mater Newcastle, Edith Street, Waratah NSW 2298, Australia

Screening identified two bisindolylmaleimides as 100 μM inhibitors of the GTPase activity of dynamin I. Focused library approaches allowed development of indole-based dynamin inhibitors called *dynoles*. 100-Fold in vitro enhancement of potency was noted with the best inhibitor, 2-cyano-3-(1-(2-(dimethylamino)-ethyl)-1*H*-indol-3-yl)-*N*-octylacrylamide (*dynole* **34**−**2**), a 1.3 ± 0.3 μM dynamin I inhibitor. Dynole **34**−**2** potently inhibited receptor mediated endocytosis (RME) internalization of Texas red-transferrin. The rank order of potency for a variety of dynole analogues on RME in U2OS cells matched their rank order for dynamin inhibition, suggesting that the mechanism of inhibition is via dynamin. Dynoles are the most active dynamin I inhibitors reported for in vitro or RME evaluations. Dynole **34**−**2** is 15-fold more active than dynasore against dynamin I and 6-fold more active against dynamin mediated RME (IC$_{50}$ ∼15 μM; RME IC$_{50}$ ∼80 μM). The dynoles represent a new series of tools to better probe endocytosis and dynamin-mediated trafficking events in a variety of cells.

Introduction

Dynamin is a large GTPase that plays a crucial role in both synaptic vesicle endocytosis and receptor mediated endocytosis, SVE[a] and RME, respectively.[1−5] It catalyzes hydrolysis of GTP to GDP, causing assembled dynamin to undergo an expansion (length) and contraction (width) that results in the fission of clathrin coated vesicles from the membrane. This mechanism has multiple biological roles and facilitates the recycling of synaptic vesicles,[2,5] the internalization of hormones and nutrients, and it is also used as a cellular entry point for viruses, toxins, and symbiotic organisms.[6] Neurotoxins botulinum and tetanus inhibit transmitter release from synapses, causing two severe neuroparalytic diseases, tetanus and botulism. Their action is dependent on their internalization via endocytosis into nerve terminals.[7]

Dynamin comprises three major isoforms: dynamin I (neurons), dynamin II (ubiquitous), and dynamin III (neurons and testes).[3,4] Common to all are four domains, a GTPase (required for vesicle fission),[3,8] pleckstrin homology (PH) (targeting domain and potentially a GTPase inhibitory module),[4] a GTPase effector domain (GED, which controls dynamin self-assembly into rings),[9,10] and a proline-rich domain (PRD) (which interacts with proteins containing an Src homology 3 (SH3) domain[3,4]

and is the site for dynamin I and III phosphorylation in vivo).[11,12] All domains are potential sites for small molecule interventions in dissecting endocytosis and potential drug targets.

Dynamin inhibitors have attracted widespread attention and have been used to study endocytosis and other aspects of membrane dynamics in a variety of cellular systems.[13−16] Small molecule inhibitors offer many distinct advantages over traditional means of dynamin inhibition in cells by expression of dynamin GTPase mutants or by small interfering RNA-mediated dynamin knockdown, which cannot readily be used to study rapid cellular effects. Small molecule, cell-permeable inhibitors are able to rapidly block endocytosis in minutes and are frequently reversible.[17,18] There is now a small but expanding "palette" of drugs available to rapidly and reversibly block dynamin I by distinct mechanisms of action: the myristoyl trimethyl ammonium bromide (MiTMAB),[18,19] Bis-tyrphostin (Bis-T),[20] room temperature ionic liquid (RTIL),[21] and dynasore[17] series of dynamin inhibitors, which are operating at different stages in its cycle of GTPase activity. For example, MiTMAB and octyl trimethyl ammonium bromide (OcTMAB) block dynamin recruitment to the cell membrane.[18]

Results

From Bisindolylmaleimides to Indoles—Simplification Improves Dynamin GTPase Inhibition. A medicinal chemistry program requires a viable lead compound. Subsequent lead optimization should facilitate the development of a more selective, potent, and less toxic analogue. The most difficult task is frequently the initial lead discovery. Most leads are derived from existing compound libraries, combinatorial libraries, or natural products. In the present study, we needed to identify a lead amenable to rapid synthetic development. Screening a number of compound libraries (data not shown) identified the structurally interesting bisindolylmaleimides (BIMs) **1** and **2** as ∼100 μM potent inhibitors of the GTPase activity of dynamin I (Figure 1). Note that **1** and **2** are pseudosymmetrical. Enzyme kinetic studies that showed BIMs **1** and **2**

* To whom correspondence should be addressed. Phone: +61 249 216486. Fax: +61 249 215472. E-mail: Adam.McCluskey@newcastle.edu.au.
† Chemistry, School of Environmental and Life Sciences, The University of Newcastle.
‡ Cell Signaling Unit, Children's Medical Research Institute, The University of Sydney.
§ Department of Medical Oncology, Calvary Mater Newcastle.
[a] Abbreviations: RME, receptor medicated endocytosis; SVE, synaptic vesicle endocytosis; GED, GTPase effector domain; PRD, proline rich domain; PH, Pleckstrin homology; SH3, Src Homology 3; MiTMAB, myristoyl trimethyl ammonium bromide; OcTMAB, octyl trimethyl ammonium bromide; Bis-T, bis-tyrphostin; RTIL, room temperature ionic liquid; BIM, bisindolylmaleimide; PKC, protein kinase C; PSA, polar surface area; U2OS, human bone osteosarcoma epithelial cells.
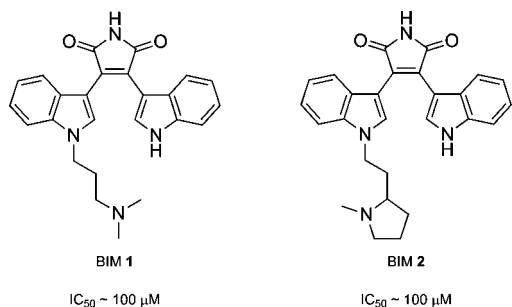
Figure 1. Lead bisindolmaleimides displaying modest levels of dynamin inhibition.
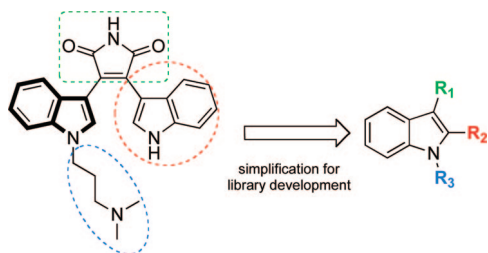

Figure 2. BIM scaffold simplification for rational design of dynamin inhibitors.

were competitive with GTP, indicating they are competitive inhibitors at the GTPase domain. BIMs of this nature are known inhibitors of protein kinase C (PKC) and glycogen synthase kinase 3.[22,23]
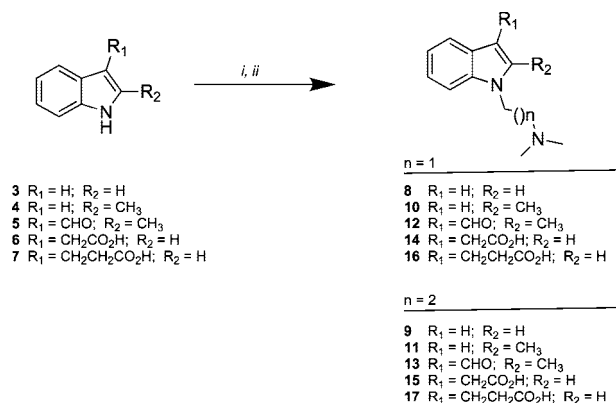
Access to a crystal or molecular modeled structure of the target protein greatly facilitates rational inhibitor development. In this particular case, while there is an apo structure of the rat GTPase domain published, it is the lack of a ligand that renders this structure unsuitable for modeling, as the GTPase domain undergoes considerable structural change upon GTP binding and GDP release.[24] There are no reports of the full-length structure of dynamin I.

There are a number of literature syntheses leading to compounds such as **1**, especially in regard to their reported inhibition of PKC.[25] However, because the goal for our study was to produce rapid access to focused compound libraries (typically 12−24 compounds per iteration), **1** was viewed as too complex.[25−30] Accordingly, we aimed to identify a minimal pharmacophore that would allow rapid, focused analogue development. Our approach to the desired compound libraries is the application of a robust focused library approach in which we placed access to compounds above synthetic elegance. Initial effort commenced by targeting the bare indole while maintaining the dimethylamino moiety (Figure 2), as this was strongly indicated from previous dynamin inhibitors we developed.[20,21]

Library 1 analogues were synthesized in a one-step procedure commencing with the treatment of five commercially available indoles (**3−7**) with NaH, and addition of either 2-chloro-*N,N*-dimethylethanamine or 3-chloro-*N,N*-dimethylpropanamine to give substituted indoles (**8−17**) in good to excellent yields (Scheme 1).

Six members of Library 1 were moderate (IC$_{50}$ > 100 ≤ 300 μM) dynamin I GTPase inhibitors (Table 1). Analogues **16** and **17** possessed additional C3-substituents and were the most active of this group at 131 ± 5 and 143 ± 7 μM, respectively. Compounds **8−11** were also active but with IC$_{50}$ values of ≥300 μM. Only analogues containing an indole-*N*-alkyl-N(CH$_3$)$_2$ moiety inhibited dynamin. Based on this, and in keeping with our focused library approach, two approaches for Library 2

Scheme 1[a]

3 R$_1$ = H; R$_2$ = H	**8** R$_1$ = H; R$_2$ = H
4 R$_1$ = H; R$_2$ = CH$_3$	**10** R$_1$ = H; R$_2$ = CH$_3$
5 R$_1$ = CHO; R$_2$ = CH$_3$	**12** R$_1$ = CHO; R$_2$ = CH$_3$
6 R$_1$ = CH$_2$CO$_2$H; R$_2$ = H	**14** R$_1$ = CH$_2$CO$_2$H; R$_2$ = H
7 R$_1$ = CH$_2$CH$_2$CO$_2$H; R$_2$ = H	**16** R$_1$ = CH$_2$CH$_2$CO$_2$H; R$_2$ = H

n = 2

9 R$_1$ = H; R$_2$ = H
11 R$_1$ = H; R$_2$ = CH$_3$
13 R$_1$ = CHO; R$_2$ = CH$_3$
15 R$_1$ = CH$_2$CO$_2$H; R$_2$ = H
17 R$_1$ = CH$_2$CH$_2$CO$_2$H; R$_2$ = H

[a] Reagents and conditions: (i) NaH, THF; (ii) 2-chloro-*N,N*-dimethylethanamine or 3-chloro-*N,N*-dimethylpropanamine.

**Table 1.** Library 1: Inhibition of Dynamin I GTPase Activity by Substituted Indoles **8−17**

Compound	R$_1$	R$_2$	R$_3$	IC$_{50}$ (μM)[a]
8	H	H	CH$_2$CH$_2$N(CH$_3$)$_2$	~300[b]
9	H	H	CH$_2$CH$_2$CH$_2$N(CH$_3$)$_2$	~300[b]
10	H	CH$_3$	CH$_2$CH$_2$N(CH$_3$)$_2$	~300[b]
11	H	CH$_3$	CH$_2$CH$_2$CH$_2$N(CH$_3$)$_2$	~300[b]
12	CHO	CH$_3$	CH$_2$CH$_2$N(CH$_3$)$_2$	−[c]
13	CHO	CH$_3$	CH$_2$CH$_2$CH$_2$N(CH$_3$)$_2$	−[c]
14	CH$_2$CO$_2$H	H	CH$_2$CH$_2$N(CH$_3$)$_2$	−[c]
15	CH$_2$CO$_2$H	H	CH$_2$CH$_2$CH$_2$N(CH$_3$)$_2$	−[c]
16	CH$_2$CH$_2$CO$_2$H	H	CH$_2$CH$_2$N(CH$_3$)$_2$	131±5
17	CH$_2$CH$_2$CO$_2$H	H	CH$_2$CH$_2$CH$_2$N(CH$_3$)$_2$	143±7

[a] IC$_{50}$ determinations are the average of at least three separate experiments, each in duplicate. [b] ~50% Inhibition at 300 μM drug concentrations, full IC$_{50}$ determination not conducted. [c] "−" No inhibition at 300 μM drug concentration.

analogues were considered (Table 2). Exploration of the available chemical space at C3 either via simple peptide coupling approaches (−CO$_2$H, **14−17**); or via Knovenangel approaches (−CHO; **12** and **13**). Given our previous Knovenangel approaches,[20,28−30] Library 2 was developed using previously reported cyanoamides (**18a−h**) (Scheme 2).[20,31−33]
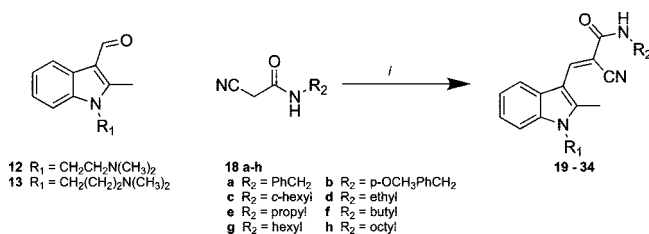
The introduction of simple chains had a marked effect on potency with C$_6$ alkyl chains substituted analogues **25** and **33**

Table 2. Library 2: Inhibition of Dynamin I GTPase Activity by Substituted Indoles **19−34**
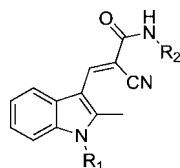
Compound	R$_1$	R$_2$	IC$_{50}$ (µM)[a]
19			196±10
20			254±19
21			~300[b]
22		-CH$_2$CH$_3$	-[c]
23		-(CH$_2$)$_2$CH$_3$	-[c]
24		-(CH$_2$)$_3$CH$_3$	~300[b]
25		-(CH$_2$)$_5$CH$_3$	7.69±2.0
26		-(CH$_2$)$_7$CH$_3$	9.05±1.7
27			201±15
28			222±22
29			~300[b]
30		-CH$_2$CH$_3$	-[c]
31		-(CH$_2$)$_2$CH$_3$	-[c]
32		-(CH$_2$)$_3$CH$_3$	-[c]
33		-(CH$_2$)$_5$CH$_3$	6.62±1.5
34-1		-(CH$_2$)$_7$CH$_3$	3.33±0.8

[a] IC$_{50}$ determinations are the average of at least three separate experiments, each in duplicate. [b] ~50% Inhibition at 300 µM drug concentrations, full IC$_{50}$ determination not conducted. [c] "−" No inhibition at 300 µM drug concentration.

Scheme 2. Library 2[a]

12 R$_1$ = CH$_2$CH$_2$N(CH$_3$)$_2$
13 R$_1$ = CH$_2$(CH$_2$)$_2$N(CH$_3$)$_2$

18 a-h
a R$_2$ = PhCH$_2$ **b** R$_2$ = p-OCH$_3$PhCH$_2$
c R$_2$ = c-hexyl   **d** R$_2$ = ethyl
e R$_2$ = propyl   **f** R$_2$ = butyl
g R$_2$ = hexyl   **h** R$_2$ = octyl

19 - 34

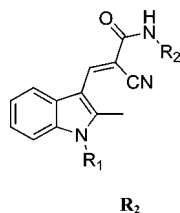[a] Reagents and conditions: (i) piperidine (cat), EtOH reflux, 3 h.

than the original lead compounds. Replacement of the alkyl side chain with a benzyl moiety causes concomitant decrease in dynamin inhibition potency (**27**, IC$_{50}$ = 201 ± 15 µM), presumably via a failure to engage a favorable hydrophobic binding interaction.

Elongation of the alkyl side chains via synthesis of analogues with C$_{10}$, C$_{12}$, and C$_{14}$ alkyl chains (**35−40**) afforded no further potency enhancements. Despite this, all C$_{10}$−C$_{14}$ analogues, **35−40**, returned inhibitory values better than the original lead compounds **1** and **2** (Table 3). This lack of improvement is not surprising, as entropic effects increase the disorder of the terminal chain. It is also possible that chain elongation begins to encroach upon a charged binding pocket, which would generate unfavorable hydrophobic-charged domain interactions and in turn encourage chain folding, preventing additional beneficial interactions and hence any increase in activity. It is also of note that the *N,N*-dimethylaminopropyl-substituted C$_{10}$, C$_{12}$, and C$_{14}$ analogues (**38−40**) are uniformly less active than the corresponding *N,N*-dimethylaminoethyl analogues (**35−37**), which suggests there is finite space available to accommodate both the indole nucleus and the long alkyl side chains and that the ultimate binding is a compromise of accommodating the pivotal *N,N*-dimethylamino moiety and the steric bulk of the alkyl chains.

The importance of the terminal *N,N*-dimethylamino moiety at N1 was examined by the synthesis of analogues shown lacking this moiety (**41−51**) and analogue **52**, which lacks only the *N,N*-dimethylamino nitrogen atom of **34−1** (IC$_{50}$ = 3.33 ± 0.75 µM) in Table 3. With these simple modifications, no changes that removed the *N,N*-dimethylamino moiety were tolerated, strongly suggesting that this is a key pharmacophoric unit for the inhibition of dynamin I by indoles of this nature.

While analogue **34** displays an excellent level of dynamin I inhibition, it is also highly lipophilic with a calculated CLogP = 5.01, on the cusp of a Lipinski violation,[34,35] suggesting good cell penetration (see below) but poor aqueous solubility. With the exception of the initial series of analogues, we did not explore the role of the indole C2−CH$_3$ substituent, but simple CLogP and polar surface area (PSA) calculations suggest that the removal of the C2−CH$_3$ will install favorable properties with LogP and PSA calculated to be 4.81 and 43.3 Å^2, respectively. Synthesis was conducted as described in Schemes 1 and 2 from indole **5**, affording the desired analogue (Figure 3).

Removal of the C2 methyl group resulted (**34−2**, Figure 3) in a 3-fold increase in potency for dynamin I inhibition (IC$_{50}$ = 1.30 ± 0.30 µM), now representing the most potent dynamin I inhibitor thus far, 2 times more potent than our existing Bis-T analogues and 15× more potent than dynasore.[17,20] This increase in potency is most likely a result of reduced steric strain and greater flexibility associated with the cyanoamide moiety and its ability to remain in the same plane as the indole nucleus. Removal of the C2−CH$_3$ moiety decreases the dihedral angle
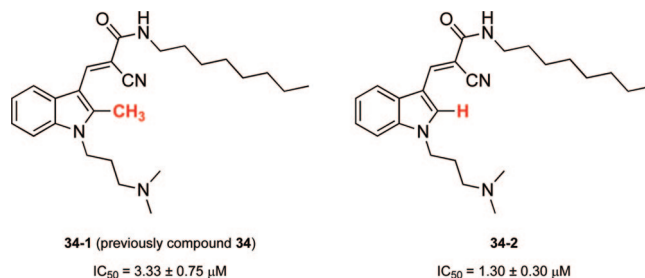
returning IC$_{50}$ values of 7.69 and 6.62 µM, respectively, and C$_8$ alkyl analogues **26** and **34** returned IC$_{50}$ values of 9.05 and 3.33 µM, respectively, which were 10−30 times more potent

Table 3. Library 3: Inhibition of Dynamin I GTPase Activity by Substituted Indoles **35−52**

Compound	R_1	R_2	IC$_{50}$ (μM)[a]
35	N (CH₂CH₂N(CH₃)₂)	-(CH$_2$)$_9$CH$_3$	10.1
36	N (CH₂CH₂N(CH₃)₂)	-(CH$_2$)$_{11}$CH$_3$	32±2
37	N (CH₂CH₂N(CH₃)₂)	-(CH$_2$)$_{13}$CH$_3$	38±1
38	(CH₂CH₂CH₂N(CH₃)₂)	-(CH$_2$)$_9$CH$_3$	30±8
39	(CH₂CH₂CH₂N(CH₃)₂)	-(CH$_2$)$_{11}$CH$_3$	42±10
40	(CH₂CH₂CH₂N(CH₃)₂)	-(CH$_2$)$_{13}$CH$_3$	52±8
41	H	benzyl	−[b]
42	H	4-methoxybenzyl	−[b]
43	H	cyclohexylmethyl	−[b]]
44	H	-CH$_2$CH$_3$	−[b]
45	H	-(CH$_2$)$_2$CH$_3$	−[b]
46	H	-(CH$_2$)$_3$CH$_3$	−[b]
47	H	-(CH$_2$)$_5$CH$_3$	−[b]
48	H	-(CH$_2$)$_7$CH$_3$	−[b]
49	H	-(CH$_2$)$_9$CH$_3$	−[b]
50	H	-(CH$_2$)$_{11}$CH$_3$	−[b]
51	H	-(CH$_2$)$_{13}$CH$_3$	−[b]
52	-(CH$_2$)$_3$CH(CH$_3$)$_2$	-(CH$_2$)$_7$CH$_3$	-

[a] IC$_{50}$ determinations are the average of at least three separate experiments, each in duplicate. [b] "−" No inhibition at 300 μM drug concentration.

Figure 3. Chemical structures and dynamin IC$_{50}$ values for dynole **34** and the C2 demethyl dynole **34**. To emphasize the structural similarity with the parent indole **34**, we have renamed these compounds dynole **34−1** and **34−2**.

associated with the cyanoamide moiety from 41.69° to 0.84°, essentially coplanar with the indole nucleus.[36]

In Vitro Inhibition of Dynamin Leads to a Complete Block in Receptor Mediated Endocytosis. Given that dynamin is essential for endocytosis, we felt it appropriate to determine the ability of our five most potent indoles, **26**, **33**, **34−1**, **34−2**, and **35**, to block RME in cells, and based on earlier efforts, we focused on human bone osteosarcoma epithelial (U2OS) cells. Using previously established approaches, we examined the effect of **26**, **33**, **34−1**, **34−2**, and **35** on the internalization of Texas Red-transferrin (Tf-TxR), which binds to the transferrin receptor and is internalized by a dynamin II-dependent pathway.[18] After

8 min of internalization under control conditions (DMSO treatment), the cells showed considerable endocytosis of Tf-TxR (Figure 4, top row) in the periphery and perinuclear region of the cell, which is typical of Tf localization in early and recycling endosomes.[37,38] After a 30 min preincubation in the presence of 30 μM of indoles **26**, **33**, **34−1**, and **35** or 10 μM of **34−2**, RME was greatly reduced (Figure 4). It is clear from Figure 4 that **26**, **33**, **34−1**, **34−2**, and **35** differ in their ability to block RME, as evidenced by the very low, but observable, levels of Tf-TxR apparent (red coloration at the periphery of the DAPI (blue) stained nucleus) with **26**, **33**, and **35**. With **34−1** and **34−2**, we note the complete or near-complete lack of color associated with Tf-TxR uptake, representing a complete block of endocytosis. Tf-TxR internalization was completely blocked at 100 μM by all five compounds (data not shown). Importantly, cell morphology was unaffected by the drug treatment, even after 30 min exposure (data not shown), indicating that there was no membrane disruption.

To quantify the effect of **26**, **33**, **34−1**, **34−2**, and **35** in U2OS cells, we used our previously reported automated quantitative RME assay based on endocytosis of Tf-A594. The IC$_{50}$ for inhibition of RME by **26** in U2OS cells was 13.2 ± 2.6 μM (Figure 5), which compares favorably with its IC$_{50}$ for dynamin I inhibition in vitro, 9.05 ± 1.68 μM. Identical trends were observed for indoles **33**, **34−1**, **34−2**, and **35**, returning IC$_{50(RME)}$ values of 14.3 ± 2.7, 10.8 ± 1.4, 5.0 ± 0.9, and 58.2 ± 11.1 μM versus IC$_{50(in\ vitro)}$s 6.62 ± 1.52, 3.33 ± 0.75, 1.30 ± 0.30, and 10.1 μM, respectively. This rank order of potency for RME inhibition closely matches the rank order of potency for inhibition of dynamin's GTPase activity, suggesting that the mechanism of inhibition is via dynamin.

Indole **34−2** represents the most potent inhibitor of dynamin mediated RME yet reported and is 15-fold more potent than dynasore in both dynamin in vitro and RME based assays.[17]

To determine whether the dynoles are toxic to cells, we assessed the viability of five fibroblast cell lines (hTert-immortalized breast stromal fibroblast, two primary skin fibroblast lines, a primary myoblast cell line, and NIH3T3 mouse fibroblasts) following 7 days of continuous exposure to dynole **34−2** using the Trypan Blue exclusion assay. Membrane integrity was not affected because >98% of cells, in all five cell lines, remained viable in the presence of dynole **34−2** (10 μM).

Mechanism of Dynamin in Vitro Inhibition. Our RME studies clearly demonstrate that indoles **26**, **33**, **34−1**, **34−2**, and **35** are efficient blockers of endocytosis, with the RME IC$_{50}$ values obtained following an identical trend for the in vitro
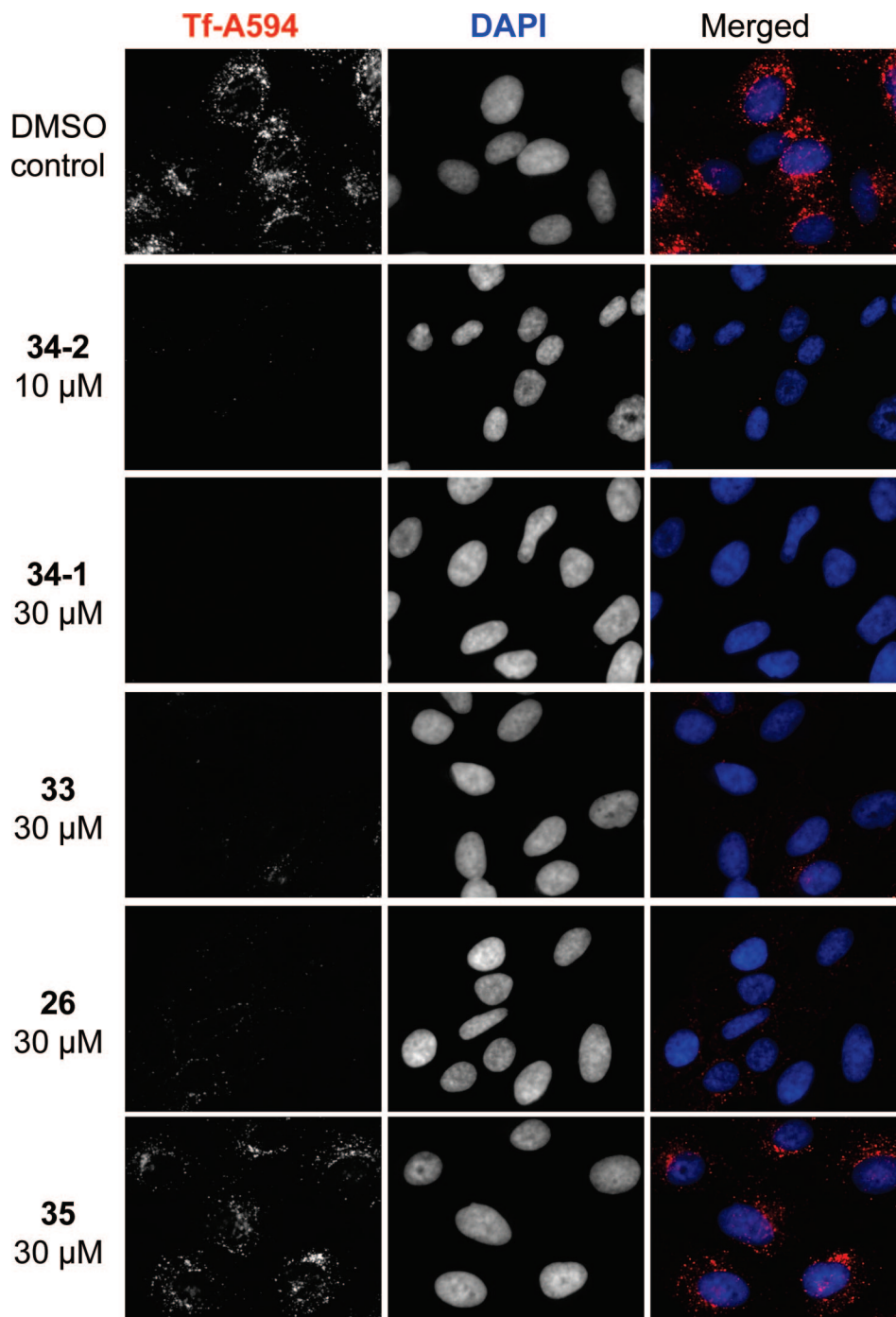
Figure 4. *Dynoles* **26**, **33**, **34**−**1**, **34**−**2**, and **35** block internalization of Tf-TxR in U2OS cells. U2OS cells were preincubated with vehicle only or different dynoles for 30 min and then incubated with Tf-TxR (A1) for 8 min at 37 °C and acid washed and fixed, and internalized Tf-TxR was detected by fluorescence microscopy (left column). Nuclei were stained blue with DAPI to show the position of the cells (middle column). The combined image (right column) shows the position of the cell nucleus (blue) and the internalized Tf-TxR (red).

inhibition of dynamin. Using traditional enzyme kinetics (Figure 6 top, bottom), we found that indole **34**−**1** is uncompetitive with GTP.

Conclusion

Synthetically simple approaches facilitated the rational design of the most potent dynamin inhibitors reported thus far. Commencing with the simplification of the bisindolylmaleimide leads, **1** and **2**, we designed and synthesized a series of small highly focused libraries exploring the structural requirements for inhibition of dynamin I GTPase. Modifications developed herein were restricted to synthetically simple approaches and

afforded new inhibitors of dynamin I displaying potency 100× that of the original lead compounds that we call the *dynole* series (*Dyn*amin inhibition by ind*oles*). Our data clearly demonstrates efficient block of endocytosis (RME), and the rank order of potency (of the *dynoles*) in blocking endocytosis correlates well with their rank potency order for dynamin I inhibition. This suggests that the observed endocytosis block is via the inhibition of dynamin GTPase activity.

Importantly, this potency is not confined to the test tube with a complete endocytic block in cells being observed with *dynoles* **34**−**1** and **34**−**2**. These analogues display high cell permeability and efficiency with cellular IC_{50}s less than an order of magnitude
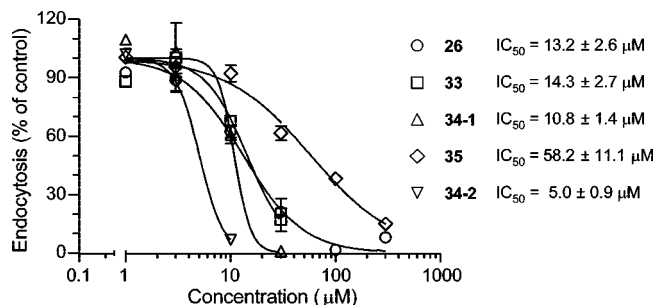
Figure 5. IC_{50} curves for endocytosis block in U2OS cells of *dynoles* **26**, **33**, **34**−**1**, **34**−**2**, and **35**. U2OS cells were preincubated with vehicle only or different dynoles for 30 min and then incubated with Tf-TxR (A1) for 8 min. Data is mean fluorescence as a percent of control cells (triplicate determinations on approximately 1200 cells each) ± SEM. The results are representative of three independent experiments.
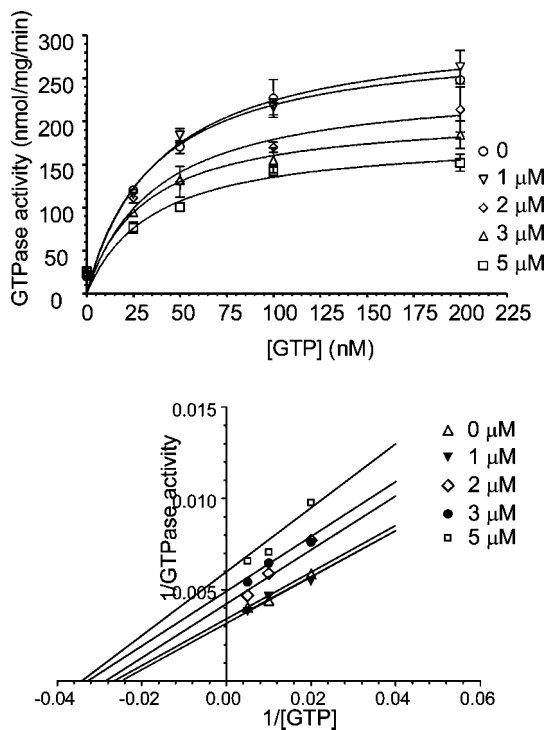

Figure 6. Kinetic analysis of interactions of dynole **34**−**1** with dynamin GTPase. Data shows this dynole is uncompetitive with GTP.

of the in vitro data. In the presence of the lead *dynole* **34**−**2**, fibroblast cells remained viable for 7 days in culture, indicating that the drug is not toxic to these cells.

The mechanism of inhibition by dynole **34**−**1** was uncompetitive. Uncompetitive inhibition is relatively unusual and can occur when an inhibitor only binds to the complex between the enzyme (dynamin) and substrate (GTP). This indicates that the dynole binds to the enzyme−substrate complex at a site other than the active site, which might be an allosteric site within the GTPase domain that becomes available upon GTP binding to dynamin.

Currently, dynasore is the primary inhibitor of dynamin mediated endocytosis in routine use.[17] The *dynoles* clearly display superior IC_{50} values and their lipophilic nature facilitates membrane permeability, evidenced by the highly efficient block of RME. These data correlate well with predicted physicochemical properties of dynole **34**−**2** with CLogP = 4.81, a polar surface area (PSA) = 41.4 Å^2, and a dipole of 5.93 debye versus CLogP = 3.65, PSA = 89.0 Å^2, and a dipole = 6.63 debye for

dynasore, suggesting a greater ease of cell penetration for the dynoles.[36] While not a pivotal consideration for the development of biochemical probes, the *dynoles* lack dynasores' catechol moiety and have lower number of hydrogen bond donor and acceptor groups, rendering this new family of dynamin inhibitors amenable for therapeutic development.[35]

We thus believe that the *dynoles*, in particular *dynole* **34**−**2**, with the synthetic ease of its access and its high dynamin I in vitro inhibition (IC_{50} = 1.30 ± 0.30 μM) and excellent ability to inhibit RME (IC_{50} = 5.0 ± 0.9 μM) represent a significant advance for the study of dynamin mediated endocytosis and will be of considerable value to researchers in the field.

Experimental Section

Biology. Materials. Phosphatidylserine (PS), phenylmethylsulfonylfluoride (PMSF), and Tween 80 were from Sigma-Aldrich (St. Louis, MO). GTP was from Roche Applied Science (Germany), leupeptin was from Bachem (Bubendorf, Switzerland). Gel electrophoresis reagents, equipment, and protein molecular weight markers were from Bio-Rad (Hercules, CA). Collagenase was from Roche. Paraformaldehyde (PFA) was from Merck Pty Ltd. (Kilsyth, Australia). Coverslips were from Lomb Scientific (Sydney, Australia). Penicillin/streptomycin, phosphate buffered salts, fetal calf serum (FCS), and Dulbecco's minimal essential medium (DMEM) were from Invitrogen (Mount Waverley, Victoria, Australia). Alexa-594 conjugated Tf (Tf-A594) and DAPI were from Molecular Probes (Oregon). All other reagents were of analytical reagent grade or better.

Drugs. Drugs were made in-house or were purchased from Sigma-Aldrich. The drugs were made up as stock solutions in 100% DMSO and diluted in 50% v/v DMSO/20 mM Tris/HCl pH 7.4 or cell media prior to further dilution in the assay. The final DMSO concentration in the GTPase or endocytosis assays was at most 3.3% or 1%, respectively. The GTPase assay for dynamin I was unaffected by DMSO up to 3.3%. Drugs were dissolved as 30 mM stocks in 100% DMSO and were light yellow in color. Stocks were stored at −20 °C for several months. They were diluted into solutions of 50% DMSO made up in 20 mM Tris/HCl pH 7.4 and then diluted again into the final assay.

Protein Production. Dynamin I was purified from sheep brain by extraction from the peripheral membrane fraction of whole brain[39] and affinity purification on GST-Amph2-SH3-sepharose as described,[40] yielding 8−10 mg of protein from 250 g of sheep brain.

Malachite Green GTPase assay. The malachite green method was used for the sensitive colorimetric detection of orthophosphate (P_i). It is based on the formation of a phosphomolybdate complex at low pH with basic dyes, causing a color change. The assay procedure is based on stimulation of native sheep brain-purified dynamin I by sonicated phosphatidylserine (PS) liposomes.[41] However, in our earlier studies, we used 200 nM dynamin I, while in the present study we used 20 nM, requiring a reformulation of assay volumes and the malachite green reagent for the present study.[19,20,41] Purified dynamin I (20 nM) (diluted in 6 mM Tris/HCl, 20 mM NaCl, 0.01% Tween 80, pH 7.4) was incubated in GTPase assay buffer (5 mM Tris/HCl, 10 mM NaCl, 2 mM Mg^{2+}, 0.05% Tween 80, pH 7.4, 1 μg/mL leupeptin, and 0.1 mM PMSF) and GTP 0.3 mM in the presence of test compound for 30 min at 37 °C. The final assay volume was 150 μL in round-bottomed 96-well plates. Plate incubations were performed in a dry heating block with shaking at 300 rpm (Eppendorf Thermomixer). Dynamin I GTPase activity was maximally stimulated by addition of different concentrations of phosphatidylserine liposomes. This assay can also be conducted in the absence of Tween with little effect on the IC_{50} values noted for the indoles listed in Figures 4−5. The reaction was terminated with 10 μL of 0.5 M EDTA pH 8.0, and the samples were stable for several hours at room temperature. To each well was added 40 μL of malachite green solution (2% w/v ammonium molybdate tetrahydrate, 0.15% w/v malachite green, and 4 M HCl: the solution was passed through 0.45 μm filters and stored in the

dark for up to 2 months at room temperature). Color was allowed to develop for 5 min (and was stable up to 2 h), and the absorbance of samples in each plate was determined on a microplate spectrophotometer at 650 nm. Phosphate release was quantified by comparison with a standard curve of sodium dihydrogen orthophosphate monohydrate (baked dry at 110 °C overnight), which was run in each experiment. GraphPad Prism 5 (GraphPad Software Inc., San Diego, CA) was used for plotting data points and analysis of enzyme kinetics using nonlinear regression. The curves were generated using the Michaelis−Menten equation $v = V_{max}[S]/(K_m + [S])$ where S = PS activator or GTP substrate. After the V_{max} and K_m values were determined, the data was transformed using the Lineweaver−Burke eq $1/v = 1/V_{max} + (K_m/V_{max})(1/[S])$.

Texas Red-Tfn Uptake. U2OS cells were cultured in DMEM supplemented with 10% FCS at 37 °C and in 5% CO_2 in a humidified incubator. Tf uptake was analyzed based on methods previously described.[41] Briefly, cells were grown in fibronectin-coated (5 μg/mL) 96-well plates. The cells were serum-starved overnight (16 h) in DMEM minus FCS. Cells were then incubated with indoles **26**, **33**, **34−1**, **34−2**, and **35** (usually 30 μM) or vehicle for 30 min prior to addition of 4 μg/mL of Tf-TxR for 8 min at 37 °C. Cell surface-bound Tf was removed by incubating the cells in an ice-cold acid wash solution (0.2 M acetic acid + 0.5 M NaCl, pH 2.8) for 10 min and was rinsed with ice-cold PBS for 5 min. Cells were immediately fixed with 4% PFA for 10 min at 37 °C. Nuclei were stained using DAPI. Quantitative analysis of the inhibition of Tf-TxR endocytosis in U2OS cells was performed on large numbers of cells by an automated acquisition and analysis system (Image Xpress Micro, Molecular Devices, Sunnyvale, CA). Nine images were collected from each well, averaging 40−50 cells per image. The average integrated intensity of Tf-TxR signal per cell was calculated for each well using IXM system and the data expressed as a percentage of control cells (vehicle treated). The average number of cells for each data point was ∼1200. IC$_{50}$ values were calculated using Graphpad Prism v5, and data was expressed as mean ± 95% confidence interval (CI) for 3 wells and ∼1200 cells.

Cell Viability Assay. Cell viability and membrane integrity was assessed by the Trypan Blue exclusion assay. Cells were seeded into 10 cm dish at a density of 1×10^5 cells per dish. On day 0 (24 h after seeding), cells were treated in the presence and absence of dynole **34−2** or vehicle control (0.5% DMSO) for 7 days. Cells (floating and adherent) were collected and cell viability was measured by Vi-CELL XR cell viability analyzer 2.03 (Beckman Coulter).

Chemistry. General Methods. THF was freshly distilled from sodium−benzophenone. Flash chromatography was carried out using silica gel 200−400 mesh (60 Å). ^{1}H and ^{13}C NMR were recorded at 300 and 75 MHz, respectively, using a Bruker Avance 300 MHz spectrometer in CDCl$_3$ and DMSO-d_6. GCMS was performed using a Shimadzu GCMS-QP2100. The instrument uses a quadrupole mass spectrometer and detects samples via electron impact ionization (EI). The University of Wollongong, Australia, Biomolecular Mass Spectrometry Laboratory, analyzed samples for HRMS. The spectra were run on the VG Autospec-oa-tof tandem high resolution mass spectrometer using CI (chemical ionization), with methane as the carrier gas and PFK (perfluorokerosene) as the reference. Microanalysis was conducted at the Microanalyis Unit at the Australian National University, Canberra, Australia. All samples returned satisfactory analyses.

(2-Indol-1-ylethyl)dimethylamine (8). To a cooled solution (0 °C) of indole (**3**) (3.0 g, 25.6 mmol) and THF (50 mL) was added slowly NaH (50% dispersion in mineral oil) (2.0 g, 41.7 mmol). This solution was allowed to stir for 30 min, then *N,N*-dimethylamino-2-chloroethane (3.2 g, 29.75 mmol) was added and the solution was heated at reflux for 70 h. Solution was allowed to cool and water added (50 mL). The organic layer was removed, and the aqueous layer extracted with ethyl acetate (2 × 50 mL). Combined organic layers were dried (MgSO$_4$) and evaporated under reduced pressure, giving orange oil. This was purified via short column chromatography DCM:MeOH (90:10). Combination of the

desired fractions and concentration under reduced pressure gave the desired product as a yellow oil, 3.50 g (70%). ^{1}H NMR (CDCl$_3$) δ 7.71 (dd, *J* = 8.5 Hz, 1.0 Hz, 1H), 7.43 (d, *J* = 8.4 Hz, 1H), 7.30 (dt, *J* = 7.0 Hz, 1.0 Hz, 1H), 7.17 (m, 2H), 6.55 (d, *J* = 3.5 Hz, 1H), 4.25 (t, *J* = 7.0 Hz, 2H), 2.64 (t, *J* = 7.0 Hz, 2H), 2.26 (s, 6H). ^{13}C NMR (CDCl$_3$) δ 135.7, 128.0, 127.3, 121.0, 120.3, 119.1, 109.1, 100.4, 56.0, 44.9, 43.8.

(3-Indol-1-ylpropyl)dimethylamine (9). Compound **9** was prepared in a similar manner to the synthesis of **8**, from indole (**3**) and 3-chloro-*N,N*-dimethylpropanamine, to give a yellow oil in a 68% yield. ^{1}H NMR (CDCl$_3$) δ 7.72 (dd, *J* = 8.4 Hz, 0.6 Hz, 1H), 7.43 (d, *J* = 8.4 Hz, 1H), 7.28 (dt, *J* = 7.0 Hz, 1.1 Hz, 1H), 7.17 (m, 2H), 6.56 (d, *J* = 3.1 Hz, 1H), 4.24 (t, *J* = 6.9 Hz, 2H), 2.31 (t, *J* = 7.0 Hz, 2H), 2.26 (s, 6H), 2.00 (quin, *J* = 6.9 Hz, 2H). ^{13}C NMR (CDCl$_3$) δ 135.6, 128.1, 127.4, 120.9, 120.4, 118.7, 108.9, 100.5, 55.9, 44.9, 43.5, 27.7.

Dimethyl-[2-(2-methylindol-1-yl)ethyl]amine (10). Compound **10** was prepared in a similar manner to the synthesis of **8**, from 2-methylindole (**4**) and 3-chloro-*N,N*-dimethylethanamine, to give a yellow oil in a 75% yield. ^{1}H NMR (CDCl$_3$) δ 7.45 (d, *J* = 7.8 Hz, 1H), 7.37 (d, *J* = 8.2 Hz, 1H), 7.10 (m, 2H), 7.00 (dt, *J* = 7.8 Hz, 0.9 Hz, 1H), 4.15 (t, *J* = 6.7 Hz, 2H), 2.56 (t, *J* = 6.7 Hz, 2H), 2.22 (s, 3H), 2.17 (s, 6H). ^{13}C NMR (75 MHz, CDCl$_3$) δ 135.9, 128.1, 126.2, 120.8, 118.4, 118.0, 109.3, 108.6, 58.6, 45.1, 43.2, 9.3.

Dimethyl-[3-(2-methylindol-1-yl)propyl]amine (11). Compound **11** was prepared in a similar manner to the synthesis of **8**, from 2-methylindole (**4**) and 3-chloro-*N,N*-dimethylpropanamine, to give a yellow oil in a 73% yield. ^{1}H NMR (CDCl$_3$) δ 7.47 (d, *J* = 7.8 Hz, 1H), 7.35 (d, *J* = 8.2, 1H), 7.10 (m, 2H), 7.00 (dt, *J* = 7.8 Hz, 1.1 Hz, 1H), 4.10 (t, *J* = 7.8 Hz, 2H), 3.35 (t, *J* = 6.9 Hz, 2H), 2.37 (s, 3H), 2.13 (t, *J* = 6.9 Hz, 2H), 2.09 (s, 6H), 1.80 (quin, *J* = 6.9 Hz, 2H). ^{13}C NMR (CDCl$_3$) δ 135.9, 128.1, 126.0, 120.8, 118.4, 117.9, 110.2, 108.6, 55.6, 45.0, 42.7, 27.8, 9.3.

1-(2-Dimethylaminoethyl)-2-methyl-1*H*-indole-3-carbaldehyde (12). Compound **12** was prepared in a similar manner to the synthesis of **8**, from 2-methylindole-3-carboxaldehyde (**5**) and 2-chloro-*N,N*-dimethylethanamine, to give, after recrystallization from ethanol, a white solid in a 78% yield; mp 50−52 °C. ^{1}H NMR (CDCl$_3$) δ 10.25 (s, 1H), 8.14 (d, *J* = 8.1 Hz, 1H), 7.43 (d, *J* = 7.5 Hz, 1H), 7.24 (m, 2H), 4.29 (t, *J* = 7.2 Hz, 2H), 2.72 (s, 3H), 2.62 (t, *J* = 7.2 Hz, 2H), 2.29 (s, 6H). ^{13}C NMR (CDCl$_3$) δ 184.4, 148.6, 136.0, 125.2, 122.4, 121.9, 119.9, 113.1 108.9, 55.7, 43.9, 40.4, 8.38.

1-(3-Dimethylaminopropyl)-2-methyl-1*H*-indole-3-carbaldehyde (13). Compound **13** was prepared in a similar manner to the synthesis of **8**, from 2-methylindole-3-carboxaldehyde (**5**) and 2-chloro-*N,N*-dimethylpropanamine, to give, after recrystallization from ethanol, an off-white solid in a 76% yield; mp 62−64 °C. ^{1}H NMR (CDCl$_3$) δ 10.08 (s, 1H), 8.10 (d, *J* = 6.6 Hz, 1H), 7.5 (d, *J* = 7.2 Hz, 1H), 7.20 (m, 2H), 4.2 (t, *J* = 7.2 Hz, 2H), 2.70 (s, 3H), 2.19 (t, *J* = 6.6 Hz, 2H), 2.12 (s, 6H), 1.83 (quin, *J* = 6.9 Hz, 2H). ^{13}C NMR (CDCl$_3$) δ 184.1, 148.7, 136.1, 125.1, 122.6, 122.1, 120.0, 113.4, 110.2, 55.6, 44.9, 40.6, 26.8, 9.72.

[1-(2-Dimethylaminoethyl)-1*H*-indol-3-yl]acetic Acid (14). Compound **12** was prepared in a similar manner to the synthesis of **8**, from 2-methyl-1*H*-indole-3-carboxylic acid (**6**) and 2-chloro-*N,N*-dimethylethanamine, to give, after recrystallization from ethanol, a white solid in a 82% yield; mp 54−56 °C. ^{1}H NMR (CDCl$_3$) δ 8.75 (br, 1H), 7.61 (d, *J* = 7.8 Hz, 1H) 7.30 (d, *J* = 7.9 Hz, 1H), 7.11 (m, 3H), 4.18 (t, *J* = 7.1 Hz, 2H), 3.83 (s, 2H), 2.38 (t, *J* = 7.1 Hz, 2H), 2.18 (s, 6H). ^{13}C NMR (75 MHz, CDCl$_3$) δ 171.6, 135.5, 126.6, 122.5, 121.4, 119.0, 118.3, 110.7, 107.7, 62.6, 55.5, 44.7, 30.1.

[1-(3-Dimethylaminopropyl)-1*H*-indol-3-yl]acetic Acid (15). Compound **15** was prepared in a similar manner to the synthesis of **8**, from 2-methyl-1*H*-indole-3-carboxylic acid (**6**) and 2-chloro-*N,N*-dimethylpropanamine, to give, after recrystallization from ethanol, a white solid in a 84% yield; mp 56−58 °C. ^{1}H NMR (300 MHz, CDCl$_3$) δ 8.71 (br, 1H), 7.62 (d, *J* = 7.6 Hz, 1H) 7.30 (d, *J* = 7.9 Hz, 1H), 7.10 (m, 3H), 4.16 (t, *J* = 6.4 Hz, 2H), 3.8 (s,

2H), 2.28 (t, *J* = 7.2 Hz, 2H), 2.18 (s, 6H), 1.80 (quin, *J* = 6.5 Hz, 2H). ^{13}C NMR (CDCl$_3$) δ 171.7, 135.7, 126.7, 122.7, 121.5, 118.9, 118.3, 110.7, 107.7, 62.6, 55.5, 44.7, 30.9, 26.3.

3-[1-(2-Dimethylaminoethyl)-2-methyl-1*H*-indol-3-yl]propionic Acid (16). Compound **16** was prepared in a similar manner to the synthesis of **8**, from 3-(2-methyl-1*H*-indol-3-yl)propanoic acid (**7**) and 2-chloro-*N*,*N*-dimethylethanamine, to give, after recrystallization from ethanol, a white solid in a 54% yield; mp 68−70 °C. ^{1}H NMR (CDCl$_3$) δ 10.60 (br, 1H), 7.48 (d, *J* = 7.9 Hz, 1H), 7.31 (d, *J* = 8.1 Hz, 1H), 7.08 (m, 2H), 6.96 (dt, *J* = 7.0, 1.1 Hz, 1H), 4.01 (t, *J* = 5.9 Hz, 2H), 2.69 (t, *J* = 7.4 Hz, 2H), 2.43 (t, *J* = 5.8 Hz, 2H), 2.32 (t, *J* = 7.3 Hz, 2H), 2.14 (s, 6H), 2.07 (s, 3H) 1.88 (quin, *J* = 7.4 Hz, 2H). ^{13}C NMR (CDCl$_3$) δ 172.7, 136.2, 127.0, 122.3, 120.7, 118.1, 118.0, 113.6, 111.2, 61.4, 57.2, 45.2, 33.2, 25.3, 23.9.

3-(1-(3-Dimethylaminopropyl)-2-methyl-1*H*-indol-3-yl)propanoic Acid (17). Compound **17** was prepared in a similar manner to the synthesis of **8** from 3-(2-methyl-1*H*-indol-3-yl)propanoic acid (**7**) and 3-chloro-*N*,*N*-dimethylpropanamine, to give, after recrystallization from ethanol, a white solid in a 60% yield; mp 74−76 °C. ^{1}H NMR (CDCl$_3$) δ 10.61 (br, 1H), 7.50 (d, *J* = 7.9 Hz, 1H), 7.31 (d, *J* = 8.1 Hz, 1H), 7.10 (m, 2H), 6.95 (dt, *J* = 7.1, 1.5 Hz, 1H), 4.01 (t, *J* = 5.9 Hz, 2H), 2.69 (t, *J* = 7.4 Hz, 2H), 2.38 (t, *J* = 5.8 Hz, 2H), 2.31 (t, *J* = 7.3 Hz, 2H), 2.14 (s, 6H), 2.07 (s, 3H) 1.88 (quin, *J* = 7.4 Hz, 2H), 1.80 (quin, *J* = 5.8 Hz, 2H). ^{13}C NMR (CDCl$_3$) δ 173.0, 137.2, 128.0, 122.7, 120.9, 118.3, 118.0, 113.9, 112.3, 61.5, 57.5, 46.1, 33.1, 25.2, 23.9, 22.8.

***N*-Benzyl-2-cyano-3-[1-(2-dimethylaminoethyl)-2-methyl-1*H*-indol-3-yl]acrylamide (19).** 1-(2-Dimethylaminoethyl)-2-methyl-1*H*-indole-3-carbaldehyde (**12**) (0.2 g, 0.87 mmol), *N*-benzyl-2-cyanoacetamide (**18a**) (0.15 g, 0.87 mmol), ethanol (5 mL), and piperidine were refluxed for 3 h. After this time, water (30 mL) was added to solution. This was then extracted with ethyl acetate (2 × 50 mL). Organic layers were combined, dried over MgSO$_4$, and concentrated under reduced pressure, giving an orange solid. This was recrystallized from MeOH giving an orange solid (82%); mp 146−148 °C. ^{1}H NMR (DMSO-d_6) δ 8.68 (t, *J* = 5.4 Hz, 1H), 8.38 (s, 1H), 7.97 (d, *J* = 7.1 Hz, 1H), 7.55 (d, *J* = 7.1 Hz, 1H), 7.12 (m, 8H), 4.42 (d, *J* = 4.3 Hz, 2H), 4.32 (t, *J* = 4.5 Hz, 2H), 2.58 (m, 5H), 2.19 (s, 6H). ^{13}C NMR (DMSO-d_6) δ 162.4, 146.1, 144.6, 139.4, 136.9, 128.2, 127.3, 126.7, 124.5, 122.4, 121.2, 121.0 118.3, 110.5, 107.6, 98.2, 57.9, 45.5, 41.1, 40.6, 11.2.

2-Cyano-*N*-(4-methoxybenzyl)-3-[1-(2-dimethylaminoethyl)-2-methyl-1*H*-indol-3-yl]-acrylamide (20). Compound **20** was prepared in a similar manner to the synthesis of **19**, substituting *N*-(4-methoxybenzyl)-2-cyanoacetamide (**18b**) for *N*-benzyl-2-cyanoacetamide (**18a**) to give, after recrystallization from methanol, an orange solid (47%); mp 165−167 °C. ^{1}H NMR (DMSO-d_6) δ 8.33 (s, 1H), 8.07 (br, 1H), 7.96 (m, 3H), 7.57 (d, *J* = 7.5 Hz, 1H), 7.22 (m, 2H), 7.12 (d, *J* = 8.7 Hz, 2H), 4.29 (t, *J* = 7.2 Hz, 2H), 3.84 (s, 3H), 2.72 (s, 3H), 2.62 (t, *J* = 7.2 Hz, 2H), 2.29 (s, 6H). ^{13}C NMR (75 MHz, DMSO-d_6) δ 162.4, 150.5, 145.5, 144.3, 136.1, 132.8, 125.2, 124.8, 122.3, 121.1, 120.7, 118.7, 114.2, 111.6, 107.6, 97.6, 58.1, 55.7, 43.9, 40.4, 11.4, 8.38.

2-Cyano-*N*-cyclohexyl-3-[1-(2-dimethylaminoethyl)-2-methyl-1*H*-indol-3-yl]acrylamide (21). Compound **21** was prepared in a similar manner to the synthesis of **21**, substituting *N*-cyclohexyl-2-cyanoacetamide (**18c**) for *N*-benzyl-2-cyanoacetamide (**18a**) to give, after recrystallization from methanol, a yellow solid (76%); mp 150−152 °C. ^{1}H NMR (DMSO-d_6) δ 8.35 (s, 1H), 8.07 (br, 1H), 7.95 (d, *J* = 7.3 Hz, 1H), 7.60 (d, *J* = 7.3 Hz, 1H), 7.21 (m, 2H), 4.28 (t, *J* = 7.2 Hz, 2H), 3.71 (m, 1H), 2.75 (s, 3H), 2.60 (t, *J* = 7.1 Hz, 2H), 2.31 (s, 6H), 1.91 (m, 2H), 1.35 (m, 2H), 1.20−1.15 (m, 4H). ^{13}C NMR (75 MHz, DMSO-d_6) δ 162.4, 145.6, 144.1, 137.5, 125.5, 122.1 121.1, 120.9, 118.1, 110.3, 108.2, 98.4, 55.6, 48.9, 43.8, 40.3, 25.5, 24.3, 24.1, 10.9.

2-Cyano-*N*-ethyl-3-[1(2-dimethylaminoethyl)-2-methyl-1*H*-indol-3-yl]acrylamide (22). Compound **22** was prepared in a similar manner to the synthesis of **19**, substituting *N*-ethyl-2-cyanoacetamide (**18d**) for *N*-benzyl-2-cyanoacetamide (**18a**) to give, after recrystallization from ethanol, a yellow solid (58%); mp 135−137

°C. ^{1}H NMR (DMSO-d_6) δ 8.33 (s, 1H), 8.07 (br, 1H), 7.96 (d, *J* = 7.2 Hz, 1H), 7.57 (d, *J* = 7.5 Hz, 1H), 7.22 (m, 2H), 4.29 (t, *J* = 7.2 Hz, 2H), 3.24 (quin, *J* = 6.6 Hz, 2H), 2.72 (s, 3H), 2.62 (t, *J* = 7.2 Hz, 2H), 2.29 (s, 6H), 1.14 (t, *J* = 7.3 Hz, 3H). ^{13}C NMR (DMSO-d_6) δ 162.2, 145.5, 144.2, 136.8, 124.5, 122.4, 121.1, 120.9, 118.3, 110.4, 107.5, 98.9, 55.7, 34.7, 43.9, 40.4, 13.6, 10.4.

2-Cyano-*N*-propyl-3-[1-(2-dimethylaminoethyl)-2-methyl-1*H*-indol-3-yl]acrylamide (23). Compound **23** was prepared in a similar manner to the synthesis of **19**, substituting *N*-propyl-2-cyanoacetamide (**18e**) for *N*-benzyl-2-cyanoacetamide (**18a**) to give, after recrystallization from ethanol, a yellow solid (54%); mp 136−138 °C. ^{1}H NMR (DMSO-d_6) δ 8.08 (s, 1H), 7.85 (br, 1H), 7.74 (d, *J* = 6.9 Hz, 1H), 7.37 (d, *J* = 6.8 Hz, 1H), 7.07 (m, 2H), 4.49 (t, *J* = 5.6 Hz, 2H), 3.49 (q, *J* = 5.8 Hz, 2H), 2.94 (s, 3H), 2.85 (t, *J* = 5.6 Hz, 2H), 2.60 (s, 6H), 1.99 (quin, *J* = 6.4 Hz, 2H) 1.42 (t, *J* = 6.5 Hz, 3H). ^{13}C NMR (DMSO-d_6) δ 162.2, 145.5, 144.2, 136.8, 124.5, 122.4, 121.1, 120.9, 118.3, 110.4, 107.5, 98.9, 57.9, 45.4, 41.7, 41.3, 22.2, 11.4, 11.3.

2-Cyano-*N*-butyl-3-[1-(2-dimethylaminoethyl)-2-methyl-1*H*-indol-3-yl] acrylamide (24). Compound **24** was prepared in a similar manner to the synthesis of **19**, substituting *N*-butyl-2-cyanoacetamide (**18f**) for *N*-benzyl-2-cyanoacetamide (**18a**) to give, after recrystallization from ethyl acetate, a yellow solid (54%); mp 137−139 °C. ^{1}H NMR (DMSO-d_6) δ 8.33 (s, 1H), 8.07 (br, 1H), 7.96 (d, *J* = 7.2 Hz, 1H), 7.57 (d, *J* = 7.5 Hz, 1H), 7.22 (m, 2H), 4.29 (t, *J* = 7.2 Hz, 2H), 3.22 (q, *J* = 6.9 Hz, 2H) 2.72 (s, 3H), 2.62 (t, *J* = 7.2 Hz, 2H), 2.29 (s, 6H), 1.48 (quin, *J* = 7.2 Hz, 2H), 1.33 (sept, *J* = 7.9 Hz, 2H), 0.89 (t, *J* = 7.2 Hz, 3H). ^{13}C NMR (DMSO-d_6) δ 162.2, 145.5, 144.2, 136.8, 124.5, 122.4, 121.1, 120.9, 118.3, 110.4, 107.5, 98.9, 55.7, 43.9, 40.4, 39.5, 25.4, 19.4, 13.0, 12.2.

2-Cyano-*N*-hexyl-3-[1(2-dimethylaminoethyl)-2-methyl-1*H*-indol-3-yl]-acrylamide (25). Compound **25** was prepared in a similar manner to the synthesis of **19**, substituting *N*-hexyl-2-cyanoacetamide (**18g**) for *N*-benzyl-2-cyanoacetamide (**18a**) to give, after recrystallization from ethyl acetate, a yellow solid (67%); mp 119−121 °C. ^{1}H NMR (300 MHz, DMSO-d_6) δ 8.25 (s, 1H), 8.10 (br, 1H), 8.00 (d, *J* = 7.1 Hz, 1H), 7.62 (d, *J* = 7.1 Hz, 1H), 7.20 (m, 2H), 4.32 (t, *J* = 7.2 Hz, 2H), 3.22 (q, *J* = 7.2 Hz, 2H), 2.70 (s, 3H), 2.59 (t, *J* = 7.2 Hz, 2H), 2.30 (s, 6H), 1.46 (quin, *J* = 7.3 Hz, 2H), 1.27 (m, 6H), 0.85 (t, *J* = 6.5 Hz, 2H); ^{13}C NMR (75 MHz, DMSO-d_6) δ 163.1, 145.2, 144.2, 136.2, 125.0, 122.3, 120.9, 19.9, 118.2, 110.4, 106.5, 99.0, 55.8, 44.1, 40.2, 38.7, 28.6, 25.8, 25.2, 21.7, 11.3.

2-Cyano-*N*-octyl-3-[1-(2-dimethylaminoethyl)-2-methyl-1*H*-indol-3-yl]-acyrlamide (26). Compound **26** was prepared in a similar manner to the synthesis of **19**, substituting *N*-octyl-2-cyanoacetamide (**18f**) for *N*-benzyl-2-cyanoacetamide (**18a**) to give, after recrystallization from ethyl acetate, a yellow solid (56%); mp 112−113 °C. ^{1}H NMR (DMSO-d_6) δ 8.30 (s, 1H), 8.10 (br, 1H), 7.99 (d, *J* = 7.0 Hz, 1H), 7.59 (d, *J* = 7.5 Hz, 1H), 7.20 (m, 2H), 4.28 (t, *J* = 7.1 Hz, 2H), 3.27 (q, *J* = 6.4 Hz, 2H), 2.74 (s, 3H), 2.62 (t, *J* = 7.2 Hz, 2H), 2.30 (s, 6H), 1.50 (quin, *J* = 6.7 Hz, 2H), 1.31 (m, 12H), 0.92 (t, *J* = 6.3 Hz, 3H). ^{13}C NMR (DMSO-d_6) δ 162.1, 144.2, 143.6, 1363, 125.5, 123.3, 121.0, 120.4, 118.3, 110.2, 107.4, 99.0, 56.7, 44.3, 41.4, 40.2, 28.9, 28.5, 26.1, 25.4, 22.1, 12.4.

2-Cyano-*N*-benzyl-3-[1-(3-dimethylaminopropyl)-2methyl-1*H*-indol-3-yl]-acrylamide (27). Compound **27** was prepared in a similar manner to the synthesis of **19** from 1-(3-dimethylaminopropyl)-2-methyl-1*H*-indole-3-carbaldehyde (**13**) and *N*-benzyl-2-cyanoacetamide (**18a**) to give, after recrystallization from ethanol, an orange solid (64%); mp 165−168 °C. ^{1}H NMR (DMSO-d_6) δ 8.58 (t, *J* = 5.4 Hz, 1H), 8.28 (s, 1H), 7.95 (d, *J* = 7.0 Hz, 1H), 7.64 (d, *J* = 7.1 Hz, 1H), 7.13−7.10 (m, 8H), 4.54 (d, *J* = 4.4 Hz, 2H), 4.20 (t, *J* = 7.0 Hz, 2H), 2.72 (s, 3H), 2.17 (t, *J* = 6.9 Hz, 2H), 2.10 (s, 6H), 1.82 (quin, *J* = 6.9 Hz, 2H). ^{13}C NMR (DMSO-d_6) δ 163.2, 146.3, 145.0, 140.4, 137.3, 128.1, 126.9, 126.5, 124.5, 122.3, 121.2, 120.8 118.2, 110.4, 108.0, 98.1, 54.3, 44.6, 40.6, 26.8, 9.9.

2-Cyano-*N*-(4-methoxybenzyl)-3-[1-(3-dimethylaminopropyl)-2-methyl-1*H*-indol-3-yl]- acrylamide (28). Compound **28** was prepared in a similar manner to the synthesis of **19** from 1-(3-dimethylaminopropyl)-2-methyl-1*H*-indole-3-carbaldehyde (**13**) and (4-methoxybenzyl)-2-cyanoacetamide (**18b**) to give, after recrystallization from ethanol, a yellow solid (74%); mp 179−180 °C. ^{1}H NMR (DMSO-*d*$_6$) δ 8.38 (s, 1H), 8.11 (br, 1H), 7.94 (m, 3H), 7.55 (d, *J* = 7.5 Hz, 1H), 7.22 (m, 2H), 7.11 (d, *J* = 8.5 Hz, 2H), 4.25 (t, *J* = 7.5 Hz, 2H), 2.73 (s, 3H), 2.17 (t, *J* = 6.7 Hz, 2H), 2.15 (s, 6H), 1.85 (quin, *J* = 6.9 Hz, 2H). ^{13}C NMR (DMSO-*d*$_6$) δ 162.5, 150.5, 146.5, 144.1, 138.1, 132.3, 127.2, 124.9, 122.3, 121.0, 120.7, 118.5, 114.1, 110.6, 108.3, 97.9, 58.0, 55.3, 44.9, 43.3, 40.2, 26.8, 11.0.

2-Cyano-*N*-cyclohexyl-3-[1-(3-dimethylaminopropyl)-2-methyl-1*H*-indol-3-yl]-acrylamide (29). Compound **29** was prepared in a similar manner to the synthesis of **19** from 1-(3-dimethylaminopropyl)-2-methyl-1*H*-indole-3-carbaldehyde (**13**) and *N*-cyclohexyl-2-cyanoacetamide (**18c**) to give, after recrystallization from ethanol, a light-yellow solid (67%); mp 163−165 °C. ^{1}H NMR (DMSO-*d*$_6$) δ 8.40 (s, 1H), 8.16 (br, 1H), 8.02 (d, *J* = 7.4 Hz, 1H), 7.67 (d, *J* = 7.5 Hz, 1H), 7.26 (m, 2H), 4.28 (t, *J* = 7.0 Hz, 2H), 3.74 (m, 1H), 2.72 (s, 3H), 2.20 (t, *J* = 7.0 Hz, 2H), 2.08 (s, 6H), 1.90 (m, 2H), 1.82 (quin, *J* = 7.0 Hz, 2H), 1.32 (m, 2H), 1.20−1.15 (m, 4H). ^{13}C NMR (DMSO-*d*$_6$) δ 162.2, 145.3, 144.0, 136.1, 125.1, 121.9, 120.8, 120.2, 118.5, 111.0, 107.1, 97.2, 55.4, 48.5, 44.5, 40.2, 31.0, 26.5, 25.0, 24.5, 23.8, 10.0.

2-Cyano-*N*-ethyl-3-[1-(3-dimethylaminopropyl)-2-methyl-1*H*-indol-3-yl]-acrylamide (30). Compound **30** was prepared in a similar manner to the synthesis of **19** from 1-(3-(dimethylamino)propyl)-2-methyl-1*H*-indole-3-carbaldehyde (**13**) and *N*-ethyl-2-cyanoacetamide (**18d**) to give, after recrystallization from ethanol, a yellow solid (57%); mp 136−138 °C. ^{1}H NMR (DMSO-*d*$_6$) δ 8.34 (s, 1H), 8.07 (br, 1H), 7.96 (d, *J* = 7.1 Hz, 1H), 7.55 (d, *J* = 7.1 Hz, 1H), 7.23 (m, 2H), 4.28 (t, *J* = 6.3 Hz, 2H), 3.20 (q, *J* = 6.2 Hz, 2H), 2.66 (s, 3H), 2.21 (m, 2H), 2.10 (s, 6H), 1.82 (t, *J* = 6.0 Hz, 2H), 1.01 (t, *J* = 7.2 Hz, 3H). ^{13}C NMR (DMSO-*d*$_6$) δ 162.0, 145.1, 144.1, 136.7, 124.3, 122.0, 119.9, 119.1, 118.2, 110.5, 107.2, 98.5, 56.0, 44.4, 39.9, 28.0, 22.1, 11.1.

2-Cyano-*N*-propyl-3-[1-(3-dimethylaminopropy)-2-methyl-1*H*-indol-3-yl]-acrylamide (31). Compound **31** was prepared in a similar manner to the synthesis of **19** from 1-(3-dimethylaminopropyl)-2-methyl-1*H*-indole-3-carbaldehyde (**13**) and *N*-propyl-2-cyanoacetamide (**18e**) to give, after recrystallization from ethanol, a yellow solid (78%); mp 142−144 °C. ^{1}H NMR (DMSO-*d*$_6$) δ 8.33 (s, 1H), 8.07 (br, 1H), 7.96 (d, *J* = 7.2 Hz, 1H), 7.57 (d, *J* = 7.5 Hz, 1H), 7.22 (m, 2H), 4.24 (t, *J* = 6.1 Hz, 2H), 3.19 (q, *J* = 6.0 Hz, 2H), 2.56 (s, 3H), 2.20 (m, 2H), 2.12 (s, 6H), 1.83 (t, *J* = 6.0 Hz; 2H), 1.53 (q, *J* = 7.1 Hz, 2H), 0.88 (t, *J* = 7.2 Hz, 3H). ^{13}C NMR (DMSO-*d*$_6$) δ 162.1, 145.2, 144.2, 136.9, 124.4, 122.2, 121.1, 120.9, 118.4, 110.5, 107.2, 98.9, 56.0, 44.9, 40.1, 28.3, 22.3, 11.3.

2-Cyano-*N*-butyl-3-[1-(3-dimethylaminopropyl)-2-methyl-1*H*-indol-3-yl]-acrylamide (32). Compound **32** was prepared in a similar manner to the synthesis of **19** from 1-(3-dimethylaminopropyl)-2-methyl-1*H*-indole-3-carbaldehyde (**13**) and *N*-butyl-2-cyanoacetamide (**18f**) to give, after recrystallization from ethanol, a yellow solid (75%); mp 124−126 °C. ^{1}H NMR (DMSO-*d*$_6$) δ 8.32 (s, 1H), 8.05 (br, 1H), 7.95 (d, *J* = 7.4 Hz, 1H), 7.57 (d, *J* = 7.5 Hz, 1H), 7.25 (m, 1H), 4.26 (t, *J* = 6.4 Hz, 2H), 3.23 (q, *J* = 5.9 Hz, 2H), 2.57 (s, 3H), 2.20 (m, 2H), 2.13 (s, 6H), 1.83 (t, *J* = 6.2 Hz, 2H), 1.49 (quin, *J* = 7.14 Hz, 2H), 1.32 (q, *J* = 7.3 Hz, 2H), 0.90 (t, *J* = 7.1 Hz, 3H). ^{13}C NMR (DMSO-*d*$_6$) δ 162.2, 145.3, 144.2, 136.8, 124.5, 122.3, 121.1, 120.9, 118.4, 110.4, 107.5, 98.8, 55.6, 44.95, 41.22, 41.0, 31.13, 26.9, 19.5, 13.6, 11.3.

2-Cyano-*N*-hexyl-3-[1-(3-dimethylaminopropyl)-2-methyl-1*H*-indol-3-yl]-acrylamide (33). Compound **33** was prepared in a similar manner to the synthesis of **19** from 1-(3-dimethylaminopropyl)-2-methyl-1*H*-indole-3-carbaldehyde (**13**) and *N*-hexyl-2-cyanoacetamide (**18g**) to give, after recrystallization from ethanol, a yellow solid (46%); mp 100−102 °C. ^{1}H NMR (DMSO-*d*$_6$) δ 8.35 (s, 1H), 8.10 (br, 1H), 7.98 (d, *J* = 7.1 Hz, 1H), 7.58 (d, *J* =

7.5 Hz, 1H), 7.21 (m, 2H), 4.25 (t, *J* = 6.2 Hz, 2H), 3.22 (q, *J* = 7.1 Hz, 2H), 2.58 (s, 3H) 2.20 (t, *J* = 6.6 Hz, 2H), 2.10 (s, 6H), 1.85 (quin, *J* = 6.9 Hz, 2H) 1.52 (quin, *J* = 7.3 Hz, 2H), 1.27 (m, 6H), 0.89 (t, *J* = 6.4 Hz, 3H). ^{13}C NMR (DMSO-*d*$_6$) δ 164.4, 147.5, 146.3, 138.0, 127.5, 124.1, 123.1, 121.7, 119.5, 112.2, 108.4, 98.6, 56.3, 45.0, 41.5, 32.0, 28.5, 27.8, 26.8, 26.0, 22.9, 14.1, 11.2, 9.7.

2-Cyano-*N*-octyl-3-[1-(3-dimethylaminopropyl)-2-methyl-1*H*-indol-3-yl]-acrylamide (34−1). Compound **34−1** was prepared in a similar manner to the synthesis of **19** from 1-(3-dimethylaminopropyl)-2-methyl-1*H*-indole-3-carbaldehyde (**13**) and *N*-octyl-2-cyanoacetamide (**18h**) to give, after recrystallization from ethanol, a yellow solid (52%); mp 99−101 °C. ^{1}H NMR (DMSO-*d*$_6$) δ 8.32 (s, 1H), 8.05 (br, 1H), 8.01 (d, *J* = 7.5 Hz, 1H), 7.55 (d, *J* = 7.5 Hz, 1H), 7.22 (m, 2H), 4.10 (t, *J* = 6.3 Hz, 2H), 3.81 (s, 2H), 3.29 (q, *J* = 6.3 Hz, 2H), 2.31 (t, *J* = 7.2 Hz, 2H), 2.20 (s, 6H), 1.85 (quin, *J* = 6.5 Hz, 2H) 1.50 (quin, *J* = 6.5 Hz, 2H), 1.25 (m, 12H), 0.80 (t, *J* = 6.3 Hz, 3H). ^{13}C NMR (DMSO-*d*$_6$) δ 163.4, 146.2, 145.1, 137.4, 126.3, 123.4, 122.4, 121.9, 119.7, 112.5, 108.4, 98.2, 56.1, 45.7, 40.6, 32.2, 28.9, 28.6, 26.9, 26.0 25.7, 25.3, 22.5, 13.5, 10.5.

2-Cyano-*N*-octyl-3-(1-(3-dimethylaminopropyl)-1*H*-indol-3-yl)-acrylamide (34−2). Compound **34−2** was prepared in a similar manner to the synthesis of **19** from 1-(3-dimethylaminopropyl)-1*H*-indole-3-carbaldehyde and *N*-octyl-2-cyanoacetamide (**18h**) to give, after recrystallization from ethanol, a yellow solid (67%); mp 105−106 °C. ^{1}H NMR (CDCl$_3$) δ 8.64 (s, 1H), 8.40 (s, 1H), 7.85 (dd, *J* = 6.8, 2.1 Hz, 1H), 7.44 (dd, *J* = 7.1, 1.6 Hz, 1H), 7.37−7.23 (m, 2H), 6.19 (t, *J* = 5.4 Hz, 1H), 4.30 (t, *J* = 6.8 Hz, 2H), 3.41 (q, *J* = 6.9 Hz, 2H), 2.22 (s, 6H), 2.07−1.94 (m, 2H), 1.59 (q, *J* = 6.96 Hz, 2H), 1.30 (m, 12H), 0.87 (t, *J* = 6.6 Hz, 3H). ^{13}C NMR (CDCl$_3$) δ 161.3, 143.3, 135.3, 132.3, 127.9, 123.0, 121.7, 119.0, 118.3, 110.0, 109.5, 94.6, 55.2, 44.8, 44.4, 39.9, 31.3, 29.1, 29.0, 28.8, 27.1, 26.4, 22.1, 13.6.

2-Cyano-*N*-decyl-3-[1-(2-dimethylaminoethyl)-2-methyl-1*H*-indol-3-yl]-acrylamide (35). Compound **35** was prepared in a similar manner to the synthesis of **19** from 1-(2-dimethylaminoethyl)-2-methyl-1*H*-indole-3-carbaldehyde (**12**) and *N*-decyl-2-cyanoacetamide to give, after recrystallization from ethyl acetate, a yellow solid (70%); mp 95−97 °C. ^{1}H NMR (DMSO-*d*$_6$) δ 8.19 (s, 1H), 7.93 (br, 1H), 7.85 (d, *J* = 7.0 Hz, 1H), 7.44 (d, *J* = 6.9 Hz, 1H), 7.10 (m, 2H), 4.32 (t, *J* = 6.9 Hz, 2H), 3.30 (q, *J* = 6.9 Hz, 2H), 2.73 (s, 3H), 2.65 (t, *J* = 6.6 Hz, 2H), 2.10 (s, 6H), 1.52 (quin, *J* = 6.8 Hz, 2H), 1.25 (m, 14H), 0.85 (t, *J* = 6.5 Hz, 3H). ^{13}C NMR (DMSO-*d*$_6$) δ 165.2, 148.6, 145.1, 138.8, 126.5, 123.0, 121.4, 121.0, 119.1, 110.1, 106.3, 100.1, 58.3, 44.7, 40.1,39.9, 30.1, 29.0, 28.7, 28.6, 28.5, 26.2, 22.1, 13.8, 10.4.

2-Cyano-*N*-dodecyl-3-[1-(2-dimethylaminoethyl)-2-methyl-1*H*-indol-3-yl]-acrylamide (36). Compound **36** was prepared in a similar manner to the synthesis of **19** from 1-(2-dimethylaminoethyl)-2-methyl-1*H*-indole-3-carbaldehyde (**12**) and *N*-dodecyl-2-cyanoacetamide to give, after recrystallization from ethyl acetate, a yellow solid (49%); mp 90−92 °C. ^{1}H NMR (CDCl$_3$) δ 8.33 (s, 1H), 7.99 (br, 1H), 7.83 (d, *J* = 6.9 Hz, 1H), 7.40 (d, *J* = 6.9 Hz, 1H), 7.00 (m, 2H), 4.30 (t, *J* = 7.3 Hz, 2H), 3.30 (q, *J* = 7.3 Hz, 2H), 2.72 (s, 3H), 2.65 (t, *J* = 7.2 Hz, 2H), 2.32 (s, 6H), 1.50 (quin, *J* = 7.0 Hz, 2H), 1.31 (m, 16H), 0.90 (t, *J* = 6.3 Hz, 3H). ^{13}C NMR (CDCl$_3$) δ 162.0, 145.0, 144.0, 135.8, 124.2, 122.1, 120.5, 119.5, 118.6, 111.0, 106.5, 96.5, 55.4, 43.9, 40.3, 31.2, 29.0, 28.7, 28.6, 26.1, 25.5, 21.4, 13.6, 11.2, 8.3.

2-Cyano-*N*-tetradecyl-3-[1-(2-dimethylaminoethyl)-2-methyl-1*H*-indol-3-yl]-acrylamide (37). Compound **37** was prepared in a similar manner to the synthesis of **19** from 1-(2-dimethylaminoethyl)-2-methyl-1*H*-indole-3-carbaldehyde (**12**) and *N*-tetradecyl-2-cyanoacetamide to give, after recrystallization from ethyl acetate, a yellow solid (56%); mp 94−96 °C. ^{1}H NMR (DMSO-*d*$_6$) δ 8.33 (s, 1H), 8.07 (br, 1H), 7.95 (d, *J* = 7.4 Hz, 1H), 7.55 (d, *J* = 7.5 Hz, 2H), 7.22 (m, 2H), 4.25 (t, *J* = 7.2 Hz, 2H), 3.19 (q, *J* = 6.3 Hz, 2H), 2.70 (s, 3H), 2.60 (t, *J* = 7.2 Hz, 2H), 2.26 (s, 6H), 1.53 (quin, *J* = 6.8 Hz, 2H), 1.30 (m, 22H), 0.88 (t, *J* = 6.3 Hz, 3H). ^{13}C NMR (DMSO-*d*$_6$) δ 165.4, 147.4, 146.4, 138.8, 126.3, 123.4,

122.8, 121.3, 120.0, 112.2, 109.3, 100.1, 58.3, 44.1, 42.4, 37.5, 29.8, 28.9, 28.7, 28.6, 26.2, 25.2, 21.1, 13.5, 8.5.

2-Cyano-*N*-decyl-3-[1-(3-dimethylaminopropyl)-2-methyl-1*H*-indol-3-yl]-acrylamide (38). Compound **38** was prepared in a similar manner to the synthesis of **19** from 1-(3-dimethylaminopropyl)-2-methyl-1*H*-indole-3-carbaldehyde (**13**) and *N*-decyl-2-cyanoacetamide to give, after recrystallization from ethyl acetate, a yellow solid (64%); mp 110−112 °C. ¹H NMR (DMSO-*d₆*) δ 8.30 (s, 1H), 8.02 (br, 1H), 7.95 (d, *J* = 7.5 Hz, 1H), 7.60 (d, *J* = 7.5 Hz, 1H), 7.25 (m, 2H), 4.26 (t, *J* = 7.2 Hz, 2H), 3.30 (q, *J* = 6.5 Hz, 2H), 2.70 (s, 3H), 2.20 (t, *J* = 6.5 Hz, 2H), 2.15 (s, 6H), 1.85 (quin, *J* = 6.5 Hz, 2H), 1.55 (quin, *J* = 6.6 Hz, 2H), 1.25 (m, 14H), 0.83 (t, *J* = 6.4 Hz, 3H). ¹³C NMR (DMSO-*d₆*) δ 163.4, 146.5, 145.1, 137.0, 125.2, 123.1, 121.4, 120.9, 119.2, 112.3, 108.1, 98.5, 56.6, 45.9, 41.6, 32.0, 30.0, 29.0, 28.9, 28.8, 28.6, 26.8, 26.2, 22.0, 12.3, 11.2.

2-Cyano-*N*-dodecyl-3-[1-(3-dimethylaminopropyl)-2-methyl-1*H*-indol-3-yl]-acrylamide (39). Compound **39** was prepared in a similar manner to the synthesis of **19** from 1-(3-dimethylaminopropyl)-2-methyl-1*H*-indole-3-carbaldehyde (**13**) and *N*-dodecyl-2-cyanoacetamide to give, after recrystallization from ethyl acetate, a yellow solid (64%); mp 103−105 °C. ¹H NMR (DMSO-*d₆*) δ 8.32 (s, 1H), 8.06 (br, 1H), 7.94 (d, *J* = 7.3 Hz, 1H), 7.50 (d, *J* = 7.5 Hz, 1H,), 7.20 (m, 2H), 4.20 (t, *J* = 7.2 Hz, 2H), 3.25 (q, *J* = 7.2 Hz, 2H,), 2.71 (s, 3H), 2.14 (t, *J* = 6.5 Hz, 2H), 2.13 (s, 6H), 1.82 (quin, *J* = 6.7 Hz, 2H), 1.50 (quin, *J* = 6.8 Hz, 2H), 1.26 (m, 16H), 0.84 (t, *J* = 6.4 Hz, 3H). ¹³C NMR (DMSO-*d₆*) δ 163.2, 146.2, 143.2, 135.3, 124.2, 123.5, 122.2, 120.5, 119.6, 112.4, 105.3, 98.4, 54.2, 44.3, 42.6, 31.6, 28.9, 28.7, 28.6, 26.8, 26.5, 25.3, 21.2, 13.0, 11.4.

2-Cyano-*N*-tetradecyl-3-[1-(2-dimethylaminoethyl)-2-methyl-1*H*-indol-3-yl]-acrylamide (40). Compound **40** was prepared in a similar manner to the synthesis of **19** from 1-(3-dimethylaminopropyl)-2-methyl-1*H*-indole-3-carbaldehyde (**13**) and *N*-tetradecyl-2-cyanoacetamide to give, after recrystallization from ethyl acetate, a yellow solid (55%); mp 99−101 °C. ¹H NMR (DMSO-*d₆*) δ 8.35 (s, 1H), 8.07 (br, 1H), 7.93 (d, *J* = 7.2 Hz, 1H), 7.57 (d, *J* = 7.5 Hz, 1H), 7.25 (m, 2H), 4.22 (t, *J* = 7.2 Hz, 2H), 3.23 (q, *J* = 6.1 Hz, 2H), 2.70 (s, 3H), 2.14 (t, *J* = 6.6 Hz, 2H), 2.05 (s, 6H), 1.82 (quin, *J* = 6.9 Hz, 2H), 1.54 (quin, *J* = 6.8 Hz, 2H), 1.30 (m, 22H), 0.88 (t, *J* = 6.4 Hz, 3H). ¹³C NMR (DMSO-*d₆*) δ 164.4, 145.5, 144.3, 136.2, 125.2, 122.2, 121.1, 120.8, 118.7, 111.5, 107.4 97.5, 55.6, 44.9, 40.3, 31.3, 29.2, 28.9, 28.7, 28.6, 26.8, 26.2, 25.3, 21.4, 13.3, 11.2.

2-Cyano-*N*-benzyl-3-(2-methyl-1*H*-indol-3-yl)-acrylamide (41). Compound **41** was prepared in a similar manner to the synthesis of **19** from 2-methyl-1*H*-indole-3-carbaldehyde (**5**) and *N*-benzyl-2-cyanoacetamide (**18a**) to give, after recrystallization from ethyl acetate, a yellow solid (52%); mp 238−240 °C. ¹H NMR (DMSO-*d₆*) δ 8.55 (t, *J* = 5.5 Hz, 1H), 8.40 (s, 1H), 8.08 (d, *J* = 7.2 Hz, 1H), 7.75 (d, *J* = 7.2 Hz, 1H), 7.10- 7.00 (m, 8H), 4.50 (d, *J* = 5.4 Hz, 2H), 2.62 (s, 3H,). ¹³C NMR (DMSO-*d₆*) δ 163.4, 146.0, 144.8, 140.4, 137.8, 128.5, 127.2, 126.5, 124.6, 123.2, 121.0, 119.0 118.4, 111.2, 108.3, 98.2, 58.1, 9.9.

2-Cyano-*N*-(4′-methoxybenzyl)-3-(2-methyl-1*H*-indol-3-yl)-acrylamide (42). Compound **42** was prepared in a similar manner to the synthesis of **19** from 2-methyl-1*H*-indole-3-carbaldehyde (**5**) and *N*-(4′-methoxybenzyl)-2-cyanoacetamide (**18b**) to give, after recrystallization from ethyl acetate, a yellow solid (47%); mp 252−254 °C. ¹H NMR (DMSO-*d₆*) δ 8.60 (t, *J* = 5.4 Hz, 1H), 8.35 (s, 1H), 7.98 (m, 3H), 7.53 (d, *J* = 7.2 Hz, 1H) 7.20 (m, 3H) 4.53 (d, *J* = 4.1 Hz, 2H), 3.91 (s, 3H), 2.54 (s, 3H). ¹³C NMR (DMSO-*d₆*) δ 163.4, 151.5, 146.5, 145.2, 138.2, 133.5, 126.1, 123.2, 122.2, 121.4, 120.4, 118.4, 115.4, 112.4, 108.5, 98.6, 59.2, 11.3.

2-Cyano-*N*-cyclohexyl-3-(2-methyl-1*H*-indol-3-yl)-acrylamide (43). Compound **43** was prepared in a similar manner to the synthesis of **19** from 2-methyl-1*H*-indole-3-carbaldehyde (**5**) and *N*-cyclohexyl-2-cyanoacetamide (**18c**) to give, after recrystallization from ethanol, a yellow solid (86%); mp 236−238 °C. ¹H NMR (DMSO-*d₆*) δ 8.30 (1H, s), 8.01 (2H, m), 7.42 (2H, d, *J* = 6.8

Hz), 7.20 (2H, m), 3.85 (1H, m), 2.67 (3H, s) 1.94 (2H, m), 1.54 (2H, m), 1.20−1.16 (4H, m). ¹³C NMR (DMSO-*d₆*) δ 162.1, 145.3, 144.2 135.8, 124.7, 124.2, 121.0, 120.5, 118.5, 110.9, 106.5, 96.8, 48.9, 31.2, 25.6, 24.8, 24.2, 12.1.

2-Cyano-*N*-ethyl-3-(2-methyl-1*H*-indol-3-yl)-acrylamide (44). Compound **44** was prepared in a similar manner to the synthesis of **19** from 2-methyl-1*H*-indole-3-carbaldehyde (**5**) and *N*-ethyl-2-cyanoacetamide (**18d**) to give, after recrystallization from ethanol, a yellow solid (66%) mp 242−244 °C. ¹H NMR (CDCl₃) δ 8.35 (1H, s), 8.02 (2H, m), 7.42 (2H, d, *J* = 6.5 Hz), 7.16 (2H, m), 3.25 (2H, quin, *J* = 6.6 Hz), 2.54 (3H, s), 1.15 (3H, t, *J* = 7.2 Hz). ¹³C NMR (CDCl₃) δ 164.2, 146.3, 145.1, 136.2, 125.2, 122.2, 121.4, 120.9, 119.9, 112.0, 103.2, 98.3, 26.2, 14.6, 11.5.

2-Cyano-*N*-propyl-3-(2-methyl-1*H*-indol-3-yl)-acrylamide (45). Compound **45** was prepared in a similar manner to the synthesis of **19** from 2-methyl-1*H*-indole-3-carbaldehyde (**5**) and *N*-propyl-2-cyanoacetamide (**18e**) to give, after recrystallization from ethanol, a yellow solid (75%); mp 245−247 °C. ¹H NMR (CDCl₃) δ 8.30 (s, 1H), 8.00 (m, 2H), 7.40 (d, *J* = 6.8 Hz, 2H), 7.15 (m, 2H), 3.20 (q, *J* = 6.5 Hz, 2H), 2.56 (s, 3H), 1.54 (sex, *J* = 7.2 Hz, 2H), 0.87 (t, *J* = 7.32 Hz, 3H). ¹³C NMR (CDCl₃) δ 162.4, 145.5, 144.3, 136.1, 125.2, 122.3, 121.1, 120.7, 118.7, 111.6, 107.6, 97.6, 41.33, 22.3, 12.7, 11.20.

2-Cyano-*N*-butyl-3-(2-methyl-1*H*-indol-3-yl)-acrylamide (46). Compound **46** was prepared in a similar manner to the synthesis of **19** from 2-methyl-1*H*-indole-3-carbaldehyde (**5**) and *N*-butyl-2-cyanoacetamide (**18f**) to give, after recrystallization from ethanol, a yellow solid (78%); mp 220−222 °C. ¹H NMR (DMSO-*d₆*) δ 8.38 (s, 1H), 8.09 (m, 2H), 7.43 (d, *J* = 7.1 Hz, 2H), 7.18 (m, 2H), 3.24 (q, *J* = 7.0 Hz, 2H), 2.60 (s, 3H), 1.49 (quin, *J* = 7.1 Hz, 2H), 1.35 (sept, *J* = 7.7 Hz, 2H), 0.92 (t, *J* = 7.1 Hz, 3H). ¹³C NMR (DMSO-*d₆*) δ 164.5, 146.2, 145.1, 138.2, 127.1, 124.2, 122.3, 121.2, 119.2, 112.6, 108.9, 99.6, 33.2, 26.3, 20.4, 13.1, 10.1.

2-Cyano-*N*-hexyl-3-(2-methyl-1*H*-indol-3-yl)-acrylamide (47). Compound **47** was prepared in a similar manner to the synthesis of **19** from 2-methyl-1*H*-indole-3-carbaldehyde (**5**) and *N*-hexyl-2-cyanoacetamide (**18g**) to give, after recrystallization from acetonitrile, a yellow solid (64%); mp 186−188 °C. ¹H NMR (DMSO-*d₆*) δ 8.32 (s, 1H), 8.02 (m, 2H), 7.45 (d, *J* = 6.9 Hz, 2H), 7.22 (m, 2H), 3.23 (q, *J* = 7.1 Hz, 2H), 2.60 (s, 3H), 1.48 (quin, *J* = 7.5 Hz, 2H), 1.29 (m, 6H), 1.0 (t, *J* = 6.7 Hz, 2H). ¹³C NMR (DMSO-*d₆*) δ 163.2, 145.2, 146.2, 137.2, 127.4 124.2, 122.3, 121.4, 119.6, 112.5, 106.2, 98.2, 32.4, 29.5, 26.8, 25.3, 22.7, 14.2, 11.5.

2-Cyano-*N*-octyl-3-(2-methyl-1*H*-indol-3-yl)-acrylamide (48). Compound **48** was prepared in a similar manner to the synthesis of **19** from 2-methyl-1*H*-indole-3-carbaldehyde (**5**) and *N*-octyl-2-cyanoacetamide (**18h**) to give, after recrystallization from acetonitrile, a yellow solid (52%); mp 174−176 °C. ¹H NMR (DMSO-*d₆*) δ 8.28 (s, 1H), 7.88 (m, 2H), 7.32 (d, *J* = 7.2 Hz, 2H), 7.10 (m, 2H), 3.30 (q, *J* = 6.8 Hz, 2H), 2.51 (s, 3H), 1.49 (quin, *J* = 6.8 Hz, 2H), 1.24 (m, 12H), 0.82 (t, *J* = 6.3 Hz, 3H). ¹³C NMR (DMSO-*d₆*) δ 161.4, 144.3, 143.2, 137.1, 124.2, 121.5, 120.1, 119.7, 117.7, 110.5, 106.6, 98.5, 30.2, 27.6, 27.5, 24.2, 24.0, 23.3, 21.0, 12.5, 9.8.

2-Cyano-*N*-decyl-3-(2-methyl-1*H*-indol-3-yl)-acrylamide (49). Compound **49** was prepared in a similar manner to the synthesis of **19** from 2-methyl-1*H*-indole-3-carbaldehyde (**5**) and *N*-decyl-2-cyanoacetamide to give, after recrystallization from acetonitrile, a yellow solid (46%); mp 166−168 °C. ¹H NMR (DMSO-*d₆*) δ 8.31 (s, 1H), 7.99 (m, 2H), 7.38 (d, *J* = 6.9 Hz, 2H), 7.13 (m, 2H), 3.25 (q, *J* = 7.0 Hz, 2H), 2.54 (s, 3H), 1.52 (quin, *J* = 6.9 Hz, 2H), 1.24 (m, 14H), 0.85 (t, *J* = 6.5 Hz, 3H); ¹³C NMR (DMSO-*d₆*) δ 165.4, 147.4, 145.3, 138.1, 127.2, 123.3, 120.9, 120.2, 117.6, 110.4, 106.2, 96.6, 31.2, 28.2, 28.0, 27.6, 27.5, 27.2, 26.2, 21.1, 12.2, 10.2.

2-Cyano-*N*-dodecyl-3-(2-methyl-1*H*-indol-3yl)-acrylamide (50). Compound **50** was prepared in a similar manner to the synthesis of **19** from 2-methyl-1*H*-indole-3-carbaldehyde (**5**) and *N*-dodecyl-2-cyanoacetamide to give, after recrystallization from acetonitrile,

a yellow solid (54%); mp 165−167 °C. ^{1}H NMR (DMSO-d_6) δ 8.27 (s, 1H), 7.96 (m, 2H), 7.35 (d, $J = 6.8$ Hz, 2H), 7.11 (m, 2H), 3.24 (q, $J = 7.0$ Hz, 2H), 2.52 (s, 3H), 1.48 (quin, $J = 6.6$ Hz, 2H), 1.25 (m, 16H), 0.84 (t, $J = 6.0$ Hz, 3H). ^{13}C NMR (DMSO-d_6) δ 162.3, 145.2, 144.0, 135.8, 125.0, 122.1, 119.7, 119.1, 117.7, 110.5, 105.2, 95.2, 30.2, 27.9, 27.7, 27.4, 26.1, 25.3, 22.2, 12.6, 9.9.

2-Cyano-N-tetradecyl-3-(2-methyl-1H-indol-3-yl)-acrylamide (51). Compound **51** was prepared in a similar manner to the synthesis of **19** from 2-methyl-1H-indole-3-carbaldehyde (**5**) and N-tetradecyl-2-cyanoacetamide to give, after recrystallization from acetonitrile, a yellow solid (45%; mp 160−162 °C. ^{1}H NMR (DMSO-d_6) δ 8.42 (s, 1H), 8.12 (m, 2H), 7.55 (d, $J = 6.8$ Hz, 2H), 7.34 (m, 2H), 3.45 (q, $J = 6.2$ Hz, 2H), 2.77 (s, 3H), 1.67 (quin, $J = 6.9$ Hz, 2H), 1.40 (m, 22H), 1.12 (t, $J = 6.4$ Hz, 3H). ^{13}C NMR (DMSO-d_6) δ 165.6, 147.2, 145.2, 138.2, 127.2, 124.1, 122.1, 121.3, 119.4, 112.5, 106.5, 98.5, 32.4, 30.0, 29.9, 28.9, 28.7, 26.4, 25.6, 22.0, 14.2, 11.1.

2-Cyano-N-octyl-3-(2-methyl-1H-indol-3-yl)-acrylamide (52). Compound **52** was prepared in a similar manner to the synthesis of **19** from 2-methyl-1-(4-methylpentyl)-1H-indole-3-carbaldehyde and N-octyl-2-cyanoacetamide (**18h**) to give, after recrystallization from ethanol, a yellow solid (86%); mp 236−238 °C. ^{1}H NMR (DMSO-d_6) δ 8.30 (s, 1H), 8.01 (m, 2H), 7.42 (d, $J = 6.8$ Hz, 2H), 7.20 (m, 2H), 3.85 (m, 1H), 2.67 (s, 3H) 1.94 (m, 2H), 1.54 (m, 2H), 1.20−1.16 (m, 4H); ^{13}C NMR (DMSO-d_6) δ 162.1, 145.3, 144.2 135.8, 124.7, 124.2, 121.0, 120.5, 118.5, 110.9, 106.5, 96.8, 48.9, 31.2, 25.6, 24.8, 24.2, 12.1.

References

(1) McLure, S. J.; Robinson, P. J. Dynamin, endocytosis and intracellular signaling. *Mol. Membr. Biol.* **1996**, *13*, 189–215.

(2) Cousin, M. A. R.; Robinson, P. J. Mechanisms of synaptic vesicle recycling illuminated by fluorescent dyes. *J. Neurochem.* **1999**, *73*, 2227–2239.

(3) Brodin, L. L. P.; Shupliakov, O. Sequential steps in clathrin-mediated synaptic vesicle endocytosis. *Curr. Opin. Neurobiol.* **2000**, *10*, 312–320.

(4) Hinshaw, J. E. Dynamin and its role in membrane fission. *Annu. Rev. Cell Dev. Biol.* **2000**, *16*, 483–519.

(5) Cousin, M. A. R.; Robinson, P. J. The dephosphins: dephosphorylation by calcineurin triggers synaptic vesicle endocytosis. *Trends Neurosci.* **2001**, *24*, 659–665.

(6) Mukherjee, S.; Ghosh, R. N.; Maxfield, F. R. Endocytosis. *Physiol. Rev.* **1997**, *77*, 759–803.

(7) Humeau, Y. D.; Grant, N. J.; Poulain, B. How botulinum and tetanus neurotoxins block neurotransmitter release. *Biochimie* **2000**, *82*, 427–446.

(8) Marks, B.; Stowell, M. H.; Vallis, Y.; Mills, I. G.; Gibson, A.; Hopkins, C. R.; McMahon, H. T. GTPase activity of dynamin and resulting conformation change are essential for endocytosis. *Nature* **2001**, *410*, 231–235.

(9) Hinshaw, J. E.; Schmind, S. L. Dynamin self-assembles into rings suggesting a mechanism for coated vesicle budding. *Nature* **1995**, *374*, 190–192.

(10) Stowell, M. H. B.; Marks, B.; Wigge, P.; McMahon, H. T. Nucleotide-dependent conformational changes in dynamin: evidence for a mechanochemical molecular spring. *Nat. Cell Biol.* **1999**, *1*, 27–32.

(11) Powell, K. A.; Valvoa, V. A.; Malladi, C. S.; Jensen, O. N.; Larsen, M. R.; Robinson, P. J. Phosphorylation of dynamin I on Ser-795 by protein kinase C blocks its association with phospholipids. *J. Biol. Chem.* **2000**, *275*, 11610–11617.

(12) Anggono, V.; Smillie, K. J.; Graham, M. E.; Valova, V. A.; Cousin, M. A.; Robinson, P. J. Syndapin I is the phosphorylation-regulated dynamin I partner in synaptic vesicle endocytosis. *Nat. Neurosci.* **2006**, *9*, 752–760.

(13) Hilliard, L. M.; Osicka, T. M.; Robinson, P. J.; Nikolic-Paterson, D. J.; Comper, W. D. Characterisation of the urinary degradation pathway in the isolated perfused rat kidney. *J. Lab. Clin. Med.* **2006**, *147*, 36–44.

(14) Newton, A. J.; Kirchhausen, T.; Murthy, V. N. Inhibition of dynamin completely blocks compensatory synaptic vesicle endocytosis. *Proc. Natl. Acad. Sci. U.S.A.* **2006**, *103*, 17955–17960.

(15) Boucrot, E.; Kirchhausen, T. Endosomal recycling controls plasma membrane area during mitosis. *Proc. Natl. Acad. Sci. U.S.A.* **2007**, *104*, 7939–7944.

(16) Xu, J.; McNeil, B.; Wu, W.; Nees, D.; Bai, L.; Wu, L. G. GTP-independent rapid and slow endocytosis at a central synapse. *Nat. Neurosci.* **2008**, *11*, 45–53.

(17) Macia, E.; Ehrlich, M.; Massol, R.; Boucrot, E.; Brunner, C.; Kirchhausen, T. Dynasore, a cell-permeable inhibitor of dynamin. *Dev. Cell* **2006**, *10*, 839–850.

(18) Quan, A. M.; McGeachie, A. B.; Keating, D. J.; van Dam, E. M.; Rusak, J.; Chau, N.; Malladi, C. S.; Chen, C.; McCluskey, A.; Cousin, M. A.; Robinson, P. J. MiTMAB is a potent dynamin inhibitor that targets the PH domain and blocks two forms of endocytosis. *Mol. Pharmacol.* **2007**, *72*, 1425–1439.

(19) Hill, T. A.; Odell, L. R.; Quan, A.; Ferguson, G.; Robinson, P. J.; McCluskey, A. Long chain amines and long chain ammonium salts as novel inhibitors of dynamin GTPase activity. *Bioorg. Med. Chem. Lett.* **2004**, *14*, 3275–3278.

(20) Hill, T.; Odell, L. R.; Edwards, J. K.; Graham, M. E.; McGeachie, A. B.; Rusak, J.; Quan, A.; Abagyan, R.; Scott, J. L.; Robinson, P. J.; McCluskey, A. Small molecule inhibitors of dynamin I GTPase activity: development of dimeric tyrphostins. *J. Med. Chem.* **2005**, *48*, 7781–7788.

(21) Zhang, J.; Lawrance, G. A.; Chau, N.; Robinson, P. J.; McCluskey, A. From Spanish fly to room temperature ionic liquids (RTILs): synthesis, thermal stability and inhibition of dynamin 1 GTPase by a novel class of RTILs. *New J. Chem.* **2008**, *32*, 28–36.

(22) Toullec, D.; Pianetti, P.; Coste, H.; Bellevergue, P.; Grand-Perret, T.; Ajakane, M.; Baudet, V.; Boissin, P.; Boursier, E.; Loriolle, F.; Duhamel, L.; Charon, D.; Kirilovsky, J. The bisindolylmaleimide GF 109203X is a potent and selective inhibitor of protein kinase C. *J. Biol. Chem.* **1991**, *266*, 15771–15781.

(23) Hers, I.; Tavare, J. M.; Denton, R. M. The protein kinase C inhibitors bisindolylmaleimide I (GF 109203x) and IX (Ro 31-8220) are potent inhibitors of glycogen synthase kinase-3 activity. *FEBS Lett.* **1999**, *460*, 433–436.

(24) Reubold, T. F.; Eschenburg, S.; Becker, A.; Leonard, M.; Schmid, S. L.; Vallee, R. B.; Kull, F. J.; Manstein, D. J. Crystal structure of the GTPase domain of rat dynamin 1. *Proc. Natl. Acad. Sci. U.S.A.* **2005**, *102*, 13093–13098.

(25) Bartlett, S. B.; Jackson, R. M.; Kayser, V.; Kilner, C.; Leach, A.; Nelson, N.; Oledzki, P. R.; Reid, G. D.; Warriner, S. L. Comparison of the ATP binding sites of protein kinases using conformationally diverse bisindolylmaleimides. *J. Am. Chem. Soc.* **2005**, *127*, 11699–11708.

(26) Wood, J. L.; Stoltz, B. M.; Dietrich, H.-J. Total synthesis of (+)- and (−)-K252a. *J. Am. Chem. Soc.* **1995**, *117*, 10413–10414.

(27) Wood, J. L.; Stoltz, B. M.; Dietrich, H.-J.; Pflum, D. A.; Petsch, D. T. Design and implementation of an efficient synthetic approach to furanosylated indolocarbazoles: total synthesis of (+)- and (−)-K252a. *J. Am. Chem. Soc.* **1997**, *119*, 9641–9651.

(28) Trost, B. M.; Krische, M. J.; Berl, V.; Grenzer, E. M. Chemo-, regio-, and enantioselective Pd-catalyzed allylic alkylation of indolocarbazole pro-aglycons. *Org. Lett.* **2002**, *4*, 2005–2008.

(29) Zhu, G. C.; Conner, S. E.; Zhou, X.; Shih, C.; Li, T.; Anderson, B. D.; Brooks, H. B.; Campbell, R. M.; Considine, E.; Dempsey, J. A.; Faul, M. M.; Ogg, C.; Patel, B.; Schultz, R. M.; Spencer, C. D.; Teicher, B.; Watkins, S. A. Synthesis, structure−activity relationship, and biological studies of indolocarbazoles as potent cyclin D1-CDK4 inhibitors. *J. Med. Chem.* **2003**, *46*, 2027–2030.

(30) Kuethe, J. T.; Wong, A.; Davies, I. W. Effective strategy for the preparation of indolocarbazole aglycons and glycosides: Total synthesis of tjipanazoles B, D, E, and I. *Org. Lett.* **2003**, *5*, 3721–3723.

(31) McCluskey, A.; Robinson, P. J.; Hill, T.; Scott, J. L.; Edwards, J. K. Green chemistry approaches to the Knoevenagel condensation: comparison of ethanol, water and solvent free (dry grind) approaches. *Tetrahedron Lett.* **2002**, *43*, 3117–3120.

(32) Correa, W. H. E.; Edwards, J. K.; McCluskey, A.; McKinnon, I.; Scott, J. L. A thermodynamic investigation of solvent-free reactions. *Green Chem.* **2003**, *5*, 30–33.

(33) Hill, T. A.; Sakoff, J. A.; Robinson, P. J.; McCluskey, A. Parallel solution-phase synthesis of targeted tyrphostin libraries with anticancer activity. *Aus. J. Chem.* **2005**, *58*, 94–103.

(34) Calculated using the *New and improved ClogP Calculator* from Chemaxon http://www.chemaxon.com (home page); http://intro.bio. umb.edu/111-112/OLLM/111F98/newclogp.html (Applet page).

(35) Lipinski, C. A.; Lombardo, F.; Dominy, B. W.; Feeney, P. J. Experimental and computational approaches to estimate solubility and permeability in drug discovery and development settings. *Adv. Drug Delivery Rev.* **1997**, *23*, 3–25.

(36) Dihedral angles were measured in Spartan 06 version 1.0.4 (for Macintosh). Wavefunction Inc., Irvine, CA, (www.wavefun.com), based on 6-31** energy minimized structures.

(37) Sheff, D.; Pelletier, L.; O'Connell, C. B.; Warren, G.; Mellman, I. Transferrin receptor recycling in the absence of perinuclear recycling endosomes. *J. Cell Biol.* **2002**, *156*, 797–804.

(38) Gaborik, Z.; Hunyady, L. Intracellular trafficking of hormone receptors. *Trends Endocrinol. Metab.* **2004**, *15*, 286–293.

(39) Robinson, P. J.; Sontag, J.-M.; Liu, J. P.; Fykse, E. M.; Slaughter, C.; McMahon, H. T.; Südhof, T. C. Dynamin GTPase regulated by protein kinase C phosphorylation in nerve terminals. *Nature* **1993**, *365*, 163–166.

(40) Quan, A.; Robinson, P. J. Rapid purification of native dynamin I and colorimetric GTPase assay. *Methods Enzymol.* **2005**, *404* (Chapter 49), 556–569.

(41) van der Bliek, A. M.; Redelmeier, T. E.; Damke, H.; Tisdale, E. J.; Meyerowitz, E. M.; Schmid, S. L. Mutations in human dynamin block an intermediate stage in coated vesicle formation. *J. Cell Biol.* **1993**, *122*, 553–563.